sensitivity are reported to decrease with age [12-14]. We have reported that some subgroups of Japanese NGT subjects show especially decreased β-cell function [15]. However, it is unclear whether deteriorated insulin secretion or insulin sensitivity is the primary factor in the increase in FPG during the period of development from NGT to IFG in Japanese.

In addition, the American Diabetes Association (ADA) lowered the cutoff value of IFG from 6.1 to 5.6 mmol/L [16]. Subjects with FPG from 5.6 to 6.1 mmol/L and with normal postprandial glucose level are categorized as having IFG in the ADA criteria, although they are categorized as having NGT in the criteria of the World Health Organization and the Japanese Diabetes Association. Thus, analysis of these subjects with mild IFG (mild impairment of fasting glucose) in view of insulin secretion and insulin sensitivity is crucial to elucidate the characteristic of subjects with borderline glucose dysregulation. To investigate the pathogenesis of prediabetes in Japanese, we compared insulin secretory capacity and insulin sensitivity in health check examinees exhibiting normal fasting glucose (NFG).

2. Subjects and methods

2.1. Subjects

Among health check examinees between 1993 and 2004 at Kyoto University Hospital, Kansai-Denryoku Hospital, and Kyoto Preventive Medical Center, 657 male subjects with FPG <6.1 mmol/L and glycated hemoglobin (HbA_{1c}) <5.6% were enrolled in the study (Table 1). Subjects with known history or signs of diabetes, previous gastrointestinal operation, liver disease, renal failure, endocrine disease, malignancy, hypertension, frequent heavy exercise, or history of medications before the study were excluded.

2.2. Measurements

Physical measurement (body height, body weight) and laboratory measurements (urine test, FPG, fasting immunoreactive insulin [F-IRI], HbA_{1c}, total cholesterol [TC], triglyceride [TG], and high-density lipoprotein cholesterol [HDL-C] level) were taken. The study was designed in compliance with the ethics regulations of the Helsinki Declaration. Blood samples were collected after overnight fasting for 16 hours [8]. Plasma glucose levels were measured by glucose oxidase method using the Hitachi Automatic Clinical Analyzer 7170 (Hitachi, Tokyo, Japan). Serum insulin levels were measured by radioimmunoassay (RIA beads II; Dainabot, Tokyo, Japan), which shows low cross-reaction with C-peptide of less than 0.005% and proinsulin less than 0.5% [8]. Glycated hemoglobin levels were measured by high-performance liquid chromatography methods. Serum TC, TG, and HDL-C levels were measured as reported previously [17]. To evaluate insulin resistance, we used the homeostasis model assessment of insulin resistance index (HOMA-IR) calculated by the formula FPG (in millimoles per liter) × IRI (in microunits per milliliter)/22.5. The HOMA-IR is a reliable measure of insulin resistance, correlating well with values obtained by glucose clamp and minimal model studies [18-20]. To calculate pancreatic β-cell function (HOMA β-cell), we used the formula 20 × IRI (in microunits per milliliter)/[FPG (in millimoles per liter) − 3.5] [18].

Table 1
Clinical characteristics of the subjects with NFG

	Data
n	657
Age (y)	44.9 ± 11.2
BMI (kg/m^2)	23.6 ± 2.8
HbA_{1c} (%)	4.8 ± 0.3
FPG (mmol/L)	5.1 ± 0.4
F-IRI (μU/mL)	5.2 ± 2.9
TC (mmol/L)	5.19 ± 0.88
TG (mmol/L)	1.45 ± 1.01
HDL-C (mmol/L)	1.45 ± 0.35

Data are mean ± SD.

2.3. Statistical analysis

Clinical data are expressed as mean ± SD. Analyses were performed using the STATVIEW 5 system (StatView, Berkeley, CA). Multiple regression analysis was used to compare age and FPG, HOMA-β, HOMA-IR, and body mass index (BMI). The same analysis was performed between HOMA-IR and BMI and TG. The NFG group was divided into low and high FPG and mild IFG, and the metabolic profiles were compared using analysis of variance. The data are expressed as mean ± SE. $P < .05$ is considered significant.

3. Results

3.1. Characteristics of the study population

As shown in Table 1, the mean age of the subjects is 44.9 ± 11.2 years and the mean BMI is 23.6 ± 2.8 kg/m^2. Among them, the number of subjects with BMI more than 30 are 22 (3.4%), concomitant with the representative epidemiologic studies in Japanese [21-23].

3.2. Correlation between age and FPG, HOMA-β, and HOMA-IR

Fig. 1A shows a positive relationship of FPG with age ($r = 0.30$, $P < .0001$; FPG [in millimoles per liter] = 0.011 × age + 4.6). Fig. 1B shows that HOMA-β has a negative correlation with age ($r = 0.24$, $P < .0001$), whereas there is no significant correlation between HOMA-IR and age ($r = 0.06$, not significant).

3.3. Correlation between HOMA-IR and BMI and serum TG levels

Fig. 2A, B shows that BMI and serum TG levels are associated with HOMA-IR ($r = 0.49$, $P < .0001$ and $r = 0.33$,

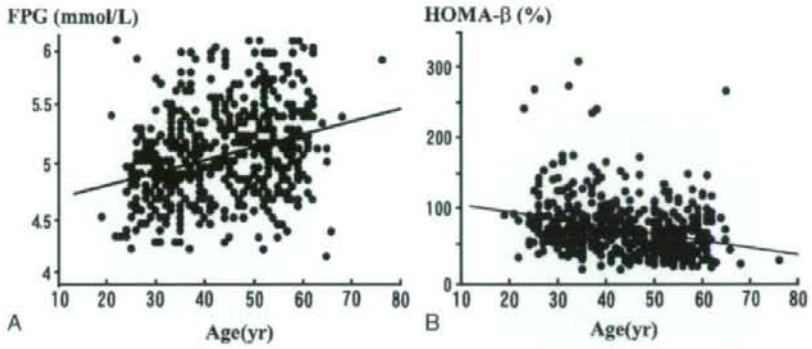

Fig. 1. Distribution of FPG (A) and HOMA-β (B) cell by age. The FPG increases with age ($r = 0.30$, $P < .0001$). The HOMA-β cell is negatively correlated with age ($r = 0.24$, $P < .0001$).

$P < .0001$, respectively). Multiple regression analysis shows that both BMI and TG are independently associated with HOMA-IR (standardized $\beta = 0.41$ and 0.15, respectively). Body mass index was the strongest determinant of HOMA-IR, and BMI did not increase with age significantly in Japanese men ($r = 0.07$, not significant).

3.4. Analysis of 3 subgroups of NFG subjects

To evaluate the factors involved in increasing FPG in Japanese NFG and the ADA recommendation of lowering the threshold of upper limit of normal FPG from 6.1 to 5.6 mmol/L [16], we divided our NFG subjects into 3 subgroups: low FPG (FPG <5.0 mmol/L), high FPG ($5.0 \le$ FPG < 5.6 mmol/L), and mild impairment of fasting glucose (mild IFG) ($5.6 \le$ FPG < 6.1 mmol/L); and age, BMI, TG, and insulin secretion and sensitivity were compared. As shown in Table 2, high FPG and mild IFG have higher age and BMI than low FPG (both $P < .0001$). Insulin in high FPG and mild IFG is increased compared with that in low FPG ($P < .001$); insulin in mild IFG is similar to that in high FPG. The HOMA-IR in high FPG and mild IFG is increased compared with that in low FPG ($P < .0001$). The HOMA-β in high FPG and mild IFG is decreased compared with that in low FPG ($P < .0001$); the HOMA-β in mild IFG is decreased compared with that in high FPG ($P < .001$).

4. Discussion

In this study, we analyzed the factors responsible for age-related elevation of FPG in Japanese men with NFG. Fasting plasma glucose was found to increase with age primarily because of reduced β-cell function rather than increased insulin resistance. In addition, we have elucidated that there was no compensatory increase in insulin secretion in mild IFG (FPG 5.6-6.1 mmol/L).

Our study subjects were composed only of men because the number of female subjects was 158, which is not comparable with male subjects. Some reports showed a difference between men and women in the elevation of FPG [24-26], and another showed similar results between men and women in the elevation of FPG [27]. We analyzed the results from our 158 female subjects, and we could not find

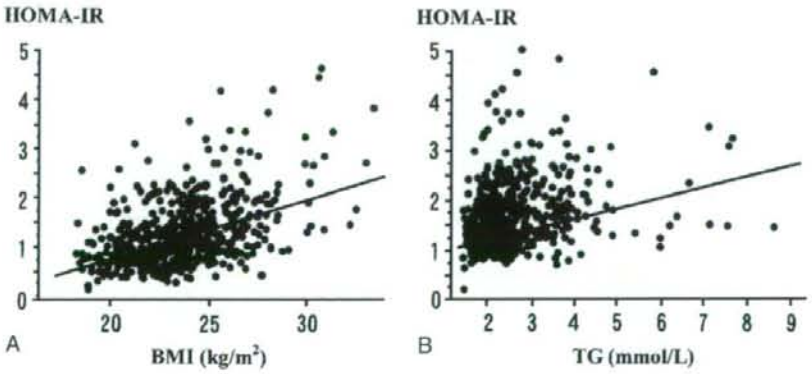

Fig. 2. Distribution of HOMA-IR by BMI (A) and TG (B). Both BMI and TG are associated with HOMA-IR (BMI: $r = 0.49$, $P < .0001$; TG: $r = 0.33$, $P < .0001$).

Table 2
Comparison of 3 FPG subgroups of NFG subjects

	Low FPG (FPG <5.0 mmol/L)	High FPG (5.0 ≤ FPG < 5.6 mmol/L)	Mild IFG (5.6 ≤ FPG < 6.1 mmol/L)
n	268	288	101
Age (y)	42.0 ± 0.7	45.7 ± 0.6[a]	49.8 ± 1.0[a,b]
BMI (kg/m^2)	23.0 ± 0.2	23.9 ± 0.1[a]	24.3 ± 0.3[a]
TC (mmol/L)	5.07 ± 0.05	5.23 ± 0.05[c]	5.35 ± 0.08[d]
TG (mmol/L)	1.30 ± 0.05	1.55 ± 0.06[d]	1.56 ± 0.09[c]
HDL-C (mmol/L)	1.45 ± 0.02	1.44 ± 0.02	1.45 ± 0.03
F-IRI (μU/mL)	4.6 ± 0.2	5.7 ± 0.2[a]	5.6 ± 0.3[e]
HOMA-IR	0.96 ± 0.04	1.31 ± 0.04[a]	1.44 ± 0.07[a]
HOMA-β (%)	78.5 ± 3.1	65.2 ± 1.9[a]	49.2 ± 2.4[a,b]

Data are mean ± SE.
[a] $P < .0001$ vs low FPG.
[b] $P < .001$ vs high FPG.
[c] $P < .05$ vs low FPG.
[d] $P < .005$ vs low FPG.
[e] $P < .0005$ vs low FPG.

remarkable differences with male subjects (data not shown). Further studies are necessary to elucidate the sex difference of the factors responsible for elevation of FPG. Although some reports showed an increase in insulin resistance in subjects older than 70 years, our male subjects were younger than 70 years. Insulin resistance in subjects older than 70 years was reported mainly because of the change in abdominal adiposity [28,29]; and in representative epidemiologic studies such as the Funagata study and the Hisayama study, the mean age of developing glucose intolerance is around 50 years in Japanese [21-23]. For these reasons, our subjects being around the age of 50 years was enough for our purpose in this study of elucidating the factors responsible for FPG elevation from normal to borderline glucose dysregulation.

Fasting plasma glucose increased by 0.011 mmol/L per year, in accord with previous reports [30]. The HOMA-β decreased by 0.85% per year, clearly indicating reduced basal insulin secretion. Although previous studies in whites and in other populations have found that insulin resistance is closely associated with age-related FPG elevation [12,31], HOMA-IR did not increase with age significantly in our subjects. To characterize the insulin resistance of our study population, we performed both simple and multiple regression analyses between HOMA-IR and the other measured factors. The BMI and serum TG levels were strongly associated with HOMA-IR ($P < .0001$), in accord with our previous results in Japanese diabetic patients [32]. Although BMI was the strongest determinant of HOMA-IR, it did not increase with age; the mean BMI of 23.6 kg/m^2 is in accord with Japanese statistical data [21-23] and is much lower than in whites [33,34]. The BMI of Asians in other studies is also reported to be lower, suggesting a common metabolic profile [35]. The leaner Japanese subjects in this study might therefore be expected to be less influenced by insulin resistance in comparison with whites.

Impaired fasting glycemia is a prediabetic state characterized by FPG elevation without increased 2h-PG. We previously reported that insulin secretory capacity and insulin sensitivity are both already decreased in IFG [8-10], suggesting the clinical importance of early deterioration of β-cell function and insulin sensitivity in developing prediabetes. In addition, we regarded the PG level of 5.6 mmol/L as an important FPG threshold value according to ADA recommendation [16]. Therefore, we compared insulin secretion and insulin sensitivity in 3 subgroups of NFG subjects: low FPG (FPG <5.0 mmol/L), high FPG (5.0 ≤ FPG < 5.6 mmol/L), and mild IFG (5.6 ≤ FPG < 6.1 mmol/L). Insulin secretion in mild IFG was not increased compared with that in high FPG, indicating impaired compensatory insulin secretion against increasing insulin resistance. Some reports have found that early-phase insulin secretion and insulin sensitivity are both decreased in NGT at a higher range of FPG (FPG >5.1-5.3 mmol/L) [36-38]. Fortunately, we could analyze 56 subjects during the 8-year follow-up period using oral glucose tolerance test results [39]. The subjects who developed from NFG to IFG showed decreasing insulin sensitivity and insulin secretory capacity, and those who developed from NFG to IGT showed decreased early insulin secretory response. These follow-up data were compatible with our previous data of IFG and IGT [5,8,10,39]. Taken together, these data indicate that insulin secretory capacity is already decreased in NGT at the higher range of FPG and that a lack of compensatory insulin secretion appears at greater than 5.6 mmol/L in FPG.

We find in Japanese NFG subjects that age-related FPG elevation is mainly due to decreased β-cell function rather than to increasing insulin resistance as in white subjects. In addition, analysis of 3 degrees of increasing FPG indicates that failure of compensatory insulin secretion is responsible for the elevation in FPG in these subjects. Thus, these data could be helpful in reconsideration of the threshold FPG for prediabetes to be recommended by the ADA [16]. However, decreasing the upper threshold of FPG entails increasing the IFG population, a costly social health problem [40]. Further studies are required to clarify the ethnic differences in the development of diabetes and diabetic complications and the value of clinical interventions in newly diagnosed IFG patients.

Acknowledgment

This study was supported in part by Health Sciences Research Grants for Comprehensive Research on Aging and Health; Research on Health Technology Assessment; and Research on Human Genome, Tissue Engineering, and Food Biotechnology from the Ministry of Health, Labour, and Welfare, and by Leading Project of Biostimulation from the Ministry of Education, Culture, Sports, Science, and Technology, Japan. We thank Use Techno, Ono Pharmaceutical, ABBOTT JAPAN, and Dainippon Pharmaceutical for their help in the study.

References

[1] Porte Jr D. Banting lecture 1990. Beta-cells in type II diabetes mellitus. Diabetes 1991;40:166-80.

[2] Lillioja S, Mott DM, Spraul M, et al. Insulin resistance and insulin secretory dysfunction as precursors of non–insulin-dependent diabetes mellitus. Prospective studies of Pima Indians. N Engl J Med 1993;329: 1988-92.

[3] DeFronzo RA. Lilly lecture 1987. The triumvirate: beta-cell, muscle, liver. A collusion responsible for NIDDM. Diabetes 1988;37:667-87.

[4] Mandavilli A, Cyranoski D. Asia's big problem. Nat Med 2004;10: 325-7.

[5] Fukushima M, Suzuki H, Seino Y. Insulin secretion capacity in the development from normal glucose tolerance to type 2 diabetes. Diabetes Res Clin Pract 2004;66:S37-43.

[6] Alberti KG, Zimmet PZ. Definition, diagnosis and classification of diabetes mellitus and its complications. Part 1: diagnosis and classification of diabetes mellitus provisional report of a WHO consultation. Diabet Med 1998;15:539-53.

[7] Suzuki H, Fukushima M, Usami M, et al. Factors responsible for development from normal glucose tolerance to isolated postchallenge hyperglycemia. Diabetes Care 2003;26:1211-5.

[8] Fukushima M, Usami M, Ikeda M, et al. Insulin secretion and insulin sensitivity at different stages of glucose tolerance: a cross-sectional study of Japanese type 2 diabetes. Metabolism 2004;53:831-5.

[9] Nishi Y, Fukushima M, Suzuki H, et al. Insulin secretion and insulin sensitivity in Japanese subjects with impaired fasting glucose and isolated fasting hyperglycemia. Diabetes Res Clin Pract 2005;70: 46-52.

[10] Izuka M, Fukushima M, Taniguchi A, et al. Factors responsible for glucose intolerance in Japanese subjects with impaired fasting glucose. Horm Metab Res 2007;39:41-5.

[11] Wiener K, Roberts NB. Age does not influence levels of HbA1c in normal subject. QJM 1999;92:169-73.

[12] Chang AM, Halter JB. Aging and insulin secretion. Am J Physiol Endocrinol Metab 2003;284:E7-E12.

[13] Paolisso G, Tagliamonte MR, Rizzo MR, et al. Advancing age and insulin resistance: new facts about an ancient history. Eur J Clin Invest 1999;29:758-69.

[14] Coon PJ, Rogus EM, Drinkwater D, et al. Role of body fat distribution in the decline in insulin sensitivity and glucose tolerance with age. J Clin Endocrinol Metab 1992;75:1125-32.

[15] Kuroe A, Fukushima M, Usami M, et al. Impaired beta-cell function and insulin sensitivity in Japanese subjects with normal glucose tolerance. Diabetes Res Clin Pract 2003;59:71-7.

[16] Report of the expert committee on the diagnosis and classification of diabetes mellitus. Diabetes Care 2003;26:S5-S20.

[17] Taniguchi A, Fukushima M, Sakai M, et al. Remnant-like particle cholesterol, triglycerides, and insulin resistance in nonobese Japanese type 2 diabetic patients. Diabetes Care 2000;23:1766-9.

[18] Bonora E, Targher G, Alberiche M, et al. Homeostasis model assessment closely mirrors the glucose clamp technique in the assessment of insulin sensitivity: studies in subjects with various degrees of glucose tolerance and insulin sensitivity. Diabetes Care 2000;23:57-63.

[19] Matthews DR, Hosker JP, Rudenski AS, et al. Homeostasis model assessment: insulin resistance and beta-cell function from fasting plasma glucose and insulin concentrations in man. Diabetologia 1985; 28:412-9.

[20] Fukushima M, Taniguchi A, Sakai M, et al. Homeostasis model assessment as a clinical index of insulin resistance. Comparison with the minimal model analysis. Diabetes Care 1999;22:1911-2.

[21] Ohmura T, Ueda K, Kiyohara Y, et al. The association of the insulin resistance syndrome with impaired glucose tolerance and NIDDM in the Japanese general population: the Hisayama study. Diabetologia 1994;37:897-904.

[22] Tominaga M, Eguchi H, Manaka H, et al. Impaired glucose tolerance is a risk factor for cardiovascular disease, but not impaired fasting glucose. The Funagata diabetes study. Diabetes Care 1999;22:920-4.

[23] Ministry of Health, Labour and Welfare Statistical database: Statistics and Information Department, second edition, chapter 1 "Public health "

[24] Williams JW, Zimmet PZ, Shaw JE, et al. Gender differences in the prevalence of impaired fasting glycaemia and impaired glucose tolerance in Mauritius. Does sex matter? Diabet Med 2003;20:915-20.

[25] Schianca GP, Castello L, Rapetti R, et al. Insulin sensitivity: gender-related differences in subjects with normal glucose tolerance. Nutr Metab Cardiovasc Dis 2006;16:339-44.

[26] Rutter MK, Parise H, Benjamin EJ, et al. Impact of glucose intolerance and insulin resistance on cardiac structure and function: sex-related differences in the Framingham Heart Study. Circulation 2003;107: 448-54.

[27] Yates AP, Laing I. Age-related increase in haemoglobin A1c and fasting plasma glucose is accompanied by a decrease in beta cell function without change in insulin sensitivity: evidence from a cross-sectional study of hospital personnel. Diabet Med 2002;19:254-8.

[28] DeNino WF, Tchernof A, Dionne IJ, et al. Contribution of abdominal adiposity to age-related differences in insulin sensitivity and plasma lipids in healthy nonobese women. Diabetes Care 2001;24:925-32.

[29] Bryhni B, Jenssen TG, Olafsen K, et al. Age or waist as determinant of insulin action? Metabolism 2003;52:850-7.

[30] Bando Y, Ushiogi Y, Okafuji K, et al. The relationship of fasting plasma glucose values and other variables to 2-h postload plasma glucose in Japanese subjects. Diabetes Care 2001;24:1156-60.

[31] Utzschneider KM, Carr DB, Hull RL, et al. Impact of intra-abdominal fat and age on insulin sensitivity and beta-cell function. Diabetes 2004; 53:2867-72.

[32] Taniguchi A, Fukushima M, Sakai M, et al. The role of the body mass index and triglyceride levels in identifying insulin-sensitive and insulin-resistant variants in Japanese non–insulin-dependent diabetic patients. Metabolism 2000;49:1001-5.

[33] Kuczmarski MF, Kuczmarski RJ, Najjar M. Effects of age on validity of self-reported height, weight, and body mass index: findings from the Third National Health and Nutrition Examination Survey, 1988-1994. J Am Diet Assoc 2001;101:28-34.

[34] Flegal KM, Carroll MD, Ogden CL, et al. Prevalence and trends in obesity among US adults, 1999-2000. JAMA 2002;288:1723-7.

[35] Qiao Q, Nakagami T, Tuomilehto J, et al. Comparison of the fasting and the 2-h glucose criteria for diabetes in different Asian cohorts. Diabetologia 2000;43:1470-5.

[36] Piche ME, Arcand-Bosse JF, Despres JP, et al. What is a normal glucose value? Differences in indexes of plasma glucose homeostasis in subjects with normal fasting glucose. Diabetes Care 2004;27:2470-7.

[37] Sato Y, Komatsu M, Katakura M, et al. Diminution of early insulin response to glucose in subjects with normal but minimally elevated fasting plasma glucose. Evidence for early beta-cell dysfunction. Diabet Med 2002;19:566-71.

[38] Godsland IF, Jeffs JA, Johnston DG. Loss of beta cell function as fasting glucose increases in the non-diabetic range. Diabetologia 2004; 47:1157-66.

[39] Mitsui R, Fukushima M, Nishi Y. Factors responsible for deteriorating glucose tolerance in newly diagnosed type 2 diabetes in Japanese men. Metabolism 2006;55:53-8.

[40] Genuth S, Alberti KG, Bennett P, et al. Follow-up report on the diagnosis of diabetes mellitus. Diabetes Care 2003;26:3160-7.

DIABETES RESEARCH AND CLINICAL PRACTICE 82 (2008) 353–358

available at www.sciencedirect.com

ScienceDirect

journal homepage: www.elsevier.com/locate/diabres

Analysis of factors influencing pancreatic β-cell function in Japanese patients with type 2 diabetes: Association with body mass index and duration of diabetic exposure

Shogo Funakoshi[a], *Shimpei Fujimoto*[a,*], *Akihiro Hamasaki*[a], *Hideya Fujiwara*[a], *Yoshihito Fujita*[a], *Kaori Ikeda*[a], *Yoshiyuki Hamamoto*[a], *Masaya Hosokawa*[a], *Yutaka Seino*[b], *Nobuya Inagaki*[a]

[a] *Department of Diabetes and Clinical Nutrition, Graduate School of Medicine, Kyoto University, 54 Shogoin Kawahara-cho, Sakyo-ku, Kyoto 606-8507, Japan*

[b] *Kansai Electric Power Hospital, Osaka, Japan*

ARTICLE INFO

Article history:
Received 19 March 2008
Received in revised form
25 August 2008
Accepted 8 September 2008
Published on line 23 October 2008

Keywords:
Type 2 diabetes
C-peptide
β-Cell
BMI
Disease duration

ABSTRACT

Aims: To elucidate the clinical factors affecting β-cell function, serum C-peptide immunoreactivity (CPR) levels of patients with type 2 diabetes were analyzed.

Methods: Seven hundred Japanese patients with type 2 diabetes were enrolled. β-Cell function was evaluated by fasting CPR (FCPR), 6 min after intravenous injection of 1 mg glucagon (CPR-6 min), and the increment of CPR (ΔCPR). Simple regression analysis between FCPR, CPR-6 min, and ΔCPR and measures of variables and stepwise multiple regression analysis were carried out.

Results: Years from diagnosis and BMI were the major independent variables predicting β-cell function. Years from diagnosis was negatively correlated with CPR-6 min ($P < 0.0001$, $r = -0.271$), and decrease in CPR-6 min was 0.050 ng/(ml year). BMI was positively correlated with CPR-6 min ($P < 0.0001$, $r = 0.369$). When subjects were divided according to BMI, the decrease in CPR-6 min per year in the high-BMI group (0.068 ng/(ml year)) was greater than that in the low-BMI group (0.035 ng/(ml year)).

Conclusion: A linear decline in endogenous insulin secretion over more than several decades of diabetes was confirmed by this cross-sectional study. The duration of diabetes exposure and BMI are thus major factors in β-cell function in Japanese patients with type 2 diabetes.

1. Introduction

Type 2 diabetes is a heterogeneous disease characterized by insulin resistance and defective insulin secretion [1], and is progressive in that therapy must be altered over time. Initially upon diagnosis, diet and exercise are generally adequate to achieve glycemic control. Oral hypoglycemic agents (OHA) are later required when patients cannot achieve glycemic control with diet and exercise. Daily insulin injection is finally indicated when patients are unable to achieve glycemic control with a combination of oral agents, diet, and exercise [2,3]. These requirements may well be, at least in part, due to progressive loss of pancreatic β-cell function. The results of the United Kingdom Prospective Diabetes Study (UKPDS) shows that pancreatic β-cell function (%β), assessed by Homeostasis Model Assessment (HOMA) in patients allocated

* *Corresponding author.* Tel.: +81 75 751 3560; fax: +81 75 751 4244.
E-mail address: fujimoto@metab.kuhp.kyoto-u.ac.jp (S. Fujimoto).

0168-8227/$ – see front matter
doi:10.1016/j.diabres.2008.09.010

to diet or OHA, decreased approximately 25% in 5 years [4]. However, the effect of more prolonged duration of diabetic exposure on β-cell function including the insulin-requiring stage has not been determined. It has been proposed that the β-cell secrets additional insulin to compensate for increasing insulin resistance to maintain normal glucose tolerance [5]. However, the effect of insulin resistance on β-cell function in diabetes remains largely unknown.

In the present study, to evaluate the clinical factors affecting β-cell function by cross-sectional study, serum C-peptide immunoreactivity levels of patients with type 2 diabetes including insulin-requiring patients were analyzed.

2. Subjects and methods

2.1. Study subjects

Seven hundred ninety-eight Japanese patients with type 2 diabetes admitted between 1997 and 2007 to Kyoto University Hospital for poor glycemic control were enrolled in the study. Type 2 diabetes mellitus was diagnosed based on the criteria of the American Diabetes Association [6]. Patients with pancreatic disease, liver disease, or those taking diabetogenic medication were excluded. Patients with serum creatinine ≥1.3 mg/dl were excluded, as serum C-peptide immunoreactivity (CPR) is elevated by decreased renal function [7]. Seven hundred patients were enrolled. Age and BMI (mean ± S.E.) were 62.2 ± 0.5 years and 24.1 ± 0.1 kg/m^2, respectively. Years from diagnosis was 11.1 ± 0.4; HbA_{1C} at admission was 9.3 ± 0.1%. Systolic and diastolic blood pressure were 122.6 ± 0.5 and 73.3 ± 0.4 mmHg, respectively. The number of patients treated with diet alone, oral hypoglycemic agents (OHA), insulin, and insulin plus OHA was 71, 225, 274, and 130, respectively.

2.2. Methods

On the first or second day in hospital, medical history, physical examination, and laboratory evaluation including glycosylated hemoglobin were performed. β-Cell function was examined within 1 week. β-Cell function was evaluated after overnight fast by glucagon test measuring CPR before [fasting CPR (FCPR)] and 6 min after intravenous injection of 1 mg glucagon (CPR-6 min) [8], as the test is valid in patients taking insulin therapy. Increment of CPR (ΔCPR) was obtained by subtracting FCPR from CPR-6 min. Serum CPR was measured by radioimmunoassay (RIA) (samples of 299 patients from 1997 to 2002 using Daiichi III, Daiichi Radioisotope Laboratories, Japan); by immunoenzymometric assay (EIA) (samples of 401 patients from 2003 to 2007 using ST AIA-PACK C-Peptide, Toso corporation, Japan). The same samples were measured by two kits, and a formula to convert the value (EIA value = 0.98 × RIA value + 0.41, $n = 161$, $r = 0.99$) was obtained. In patients taking OHA, medication was stopped for the glucagon test, but was maintained until 1 day before to prevent hyperglycemia during the test. Fasting plasma glucose was measured by glucose oxidase method when the glucagon test was performed. The date of diagnosis for patients was determined from their medical record, medical history, and previous clinical data by the criteria for the diagnosis of diabetes proposed by the American Diabetes Association [6].

2.3. Statistical analysis

Statistical analysis was performed with the StatView 5.0 system (SAS institute Inc., Cary, NC). Data are presented as mean ± S.E. The relationship between the parametric clinical data and CPR values was investigated by Pearson analysis. The relationship between the nonparametric clinical data and CPR values was investigated by Spearman analysis. Stepwise multiple regression analysis was performed. Clinical parameters among the three groups above were compared by analysis of variance (ANOVA). For comparison of two groups, Scheffe's test was performed as post hoc analysis. P values <0.05 were considered statistically significant.

3. Results

Simple correlation coefficients between FCPR, CPR-6 min, and ΔCPR and measures of variables (age, years from diagnosis, BMI, HbA_{1C}, systolic and diastolic blood pressure, serum creatinine, sex, and fasting plasma glucose) were calculated and are indicated in Table 1. Stepwise multiple regression analysis was carried out using independent variables in Table 1 to predict indexes of endogenous insulin secretion as a dependent variable (Table 2). Stepwise multiple regression analysis is indicated in Table 2. FCPR was independently predicted by years from diagnosis, BMI, and serum creatinine,

Table 1 – P value of simple correlation between indexes of endogenous insulin secretion and measures of variables.

	FCPR (ng/ml)	CPR-6 min (ng/ml)	ΔCPR (ng/ml)
Age (year)	0.0326	<0.0001	<0.0001
Years from diagnosis	<0.0001	<0.0001	<0.0001
BMI (kg/m^2)	<0.0001	<0.0001	<0.0001
Systolic blood pressure (mmHg)	0.9481	0.2091	0.0593
Diastolic blood pressure (mmHg)	0.1139	0.0044	0.0016
FPG (mg/dl)	0.0783	0.0010	0.0002
HbA_{1C} (%)	0.0375	0.2152	0.7699
sCre (mg/dl)	<0.0001	0.0836	0.3917
Sex	0.8978	0.7958	0.8206

FPG: fasting plasma glucose; sCre: serum creatinine.

Table 2 – Stepwise multiple regression analysis for predictors of indexes of endogenous insulin secretion.

	F value	Partial regression coefficient	Standard partial regression coefficient	R^2 (|R|)
FCPR (ng/ml)				
Years from diagnosis	41.4	−0.020	−0.219	0.217 (0.469)
BMI (kg/m^2)	114.4	0.087	0.362	
sCre (mg/dl)	27.7	0.877	0.179	
CPR-6 min (ng/ml)				
Years from diagnosis	45.8	−0.043	−0.233	0.198 (0.449)
BMI (kg/m^2)	102.8	0.167	0.348	
FPG (mg/dl)	10.8	0.004	0.113	
ΔCPR (ng/ml)				
Years from diagnosis	34.7	−0.025	−0.212	0.129 (0.365)
BMI (kg/m^2)	47.9	0.077	0.248	
FPG (mg/dl)	13.2	0.003	0.130	

FPG: fasting plasma glucose; sCre: serum creatinine.

accounting for 21.7% of the variability of FCPR. CPR-6 min and ΔCPR were independently predicted by years from diagnosis, BMI, and fasting plasma glucose (FPG), accounting for 19.8% and 12.9% of the variability of the dependent variables, respectively.

Scattered plots of linear regression, simple regression coefficient, and formula between indexes of endogenous insulin secretion and years from diagnosis, BMI, FPG, and serum creatinine are shown in Figs. 1–4, respectively.

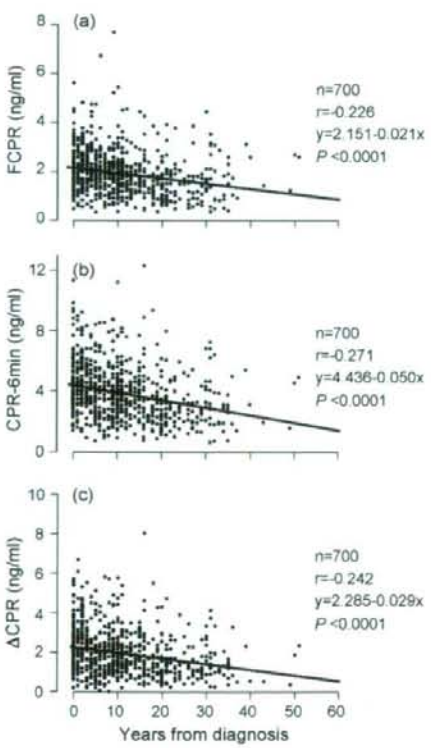

Fig. 1 – The relationship between years from diagnosis and FCPR (a), CPR-6 min (b), and ΔCPR (c).

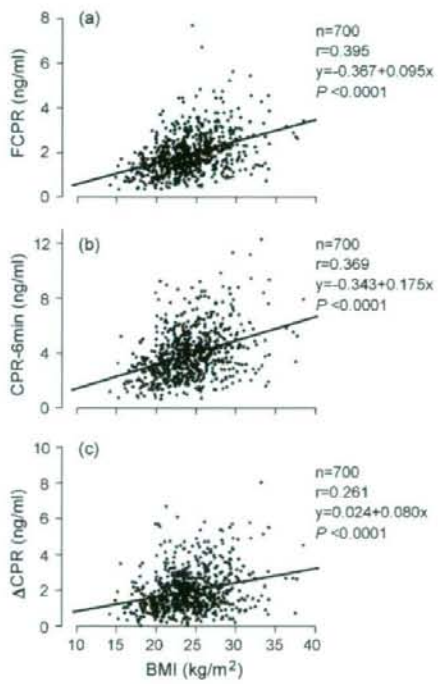

Fig. 2 – The relationship between BMI and FCPR (a), CPR-6 min (b), and ΔCPR (c).

Years from diagnosis was negatively correlated with FCPR ($P < 0.0001$, $r = -0.226$), CPR-6 min ($P < 0.0001$, $r = -0.271$), and ΔCPR ($P < 0.0001$, $r = -0.242$) (Fig. 1). The decrease in FCCP, CPR-6 min, and ΔCPR was 0.021, 0.050, and 0.029 ng/(ml year), respectively (Fig. 1). BMI was positively correlated with FCPR ($P < 0.0001$, $r = 0.395$), CPR-6 min ($P < 0.0001$, $r = 0.369$), and ΔCPR ($P < 0.0001$, $r = 0.261$) (Fig. 2). FPG was weakly correlated with CPR-6 min ($P = 0.001$, $r = 0.125$) and ΔCPR ($P = 0.0002$, $r = 0.141$) (Fig. 3). Serum creatinine was weakly correlated with FCPR ($P < 0.0001$, $r = 0.171$) (Fig. 4).

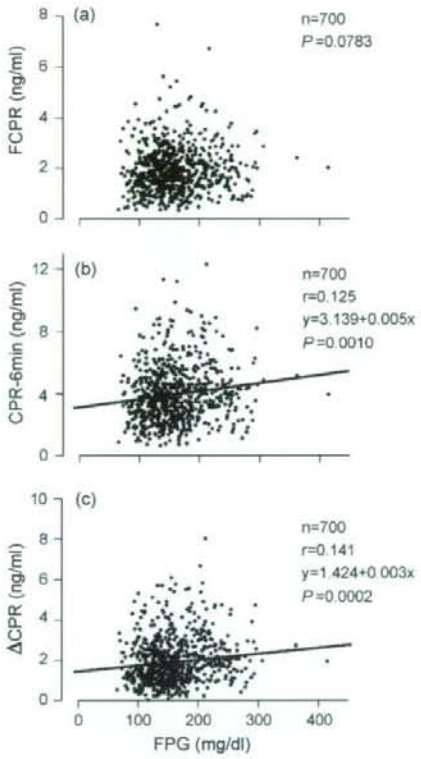

Fig. 3 – The relationship between fasting plasma glucose (FPG) and FCPR (a), CPR-6 min (b), and ΔCPR (c).

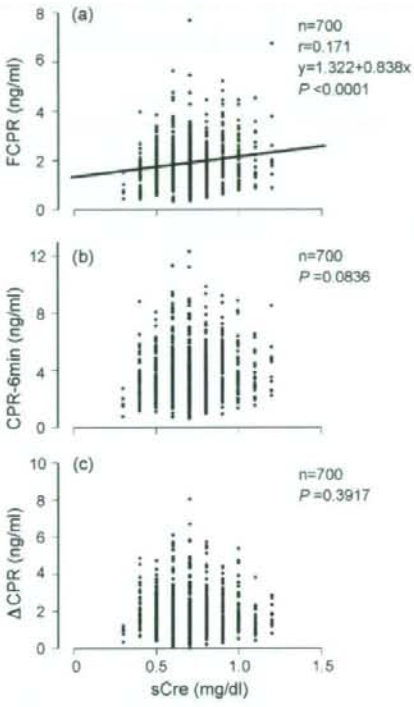

Fig. 4 – The relationship between serum creatinine (sCre) and FCPR (a), CPR-6 min (b), and ΔCPR (c).

Because BMI is the other major independent variable associated with indexes of endogenous insulin secretion, we compared the subjects divided at BMI 25.0. Single regression analysis between CPR-6 min and years from diagnosis was performed on each group. Years from diagnosis was negatively correlated with CPR-6 min in both groups (BMI < 25: $n = 430$, $P < 0.0001$, $r = -0.233$, $y = 3.876 - 0.035x$; BMI ≥ 25.0: $n = 270$, $P < 0.0001$, $r = -0.309$, $y = 5.229 - 0.067x$). The decrease in CPR-6 min per year in the high-BMI (27.9 ± 0.2 kg/m^2) group (0.067 ng/(ml year)) was greater than that in the low-BMI (21.8 ± 0.1 kg/m^2) group (0.035 ng/(ml year)). Comparison of the clinical data among four groups of increasing years from

Table 3 – Comparison of clinical characteristics and clinical profile among groups according to years from diagnosis.

Groups (years from diagnosis)	I (–9.9)	II (10.0–19.9)	III (20.0–29.9)	IV (30–)	P
Years from diagnosis	3.6 ± 0.2	13.3 ± 0.2[a]	23.4 ± 0.3[a,b]	34.0 ± 0.7[a,b,c]	<0.0001
Number of subjects	355	204	94	47	
Sex (M/F)	215/140	114/90	50/44	31/16	
Age (year)	58.4 ± 0.7	63.7 ± 0.8[a]	68.8 ± 0.9[a,b]	70.9 ± 1.2[a,b]	<0.0001
BMI (kg/m^2)	24.4 ± 0.2	24.0 ± 0.3	23.3 ± 0.3	23.9 ± 0.5	0.0912
HbA_{1c} (%)	9.5 ± 0.1	9.1 ± 0.1	9.4 ± 0.2	8.9 ± 0.2	0.0823
SBP (mmHg)	122.0 ± 0.7	122.1 ± 0.9	124.8 ± 1.5	124.8 ± 2.1	0.2163
DBP (mmHg)	75.3 ± 0.5	72.0 ± 0.6[a]	69.9 ± 0.9[a]	70.8 ± 1.3[a]	<0.0001
sCre (mg/dl)	0.70 ± 0.01	0.72 ± 0.01	0.73 ± 0.02	0.76 ± 0.03	0.0650
FPG (mg/dl)	162.9 ± 2.6	159.7 ± 3.4	154.6 ± 4.9	156.1 ± 7.5	0.4498
FCPR (ng/ml)	2.12 ± 0.05	1.83 ± 0.06[a]	1.46 ± 0.08[a,b]	1.73 ± 0.14[a]	<0.0001
CPR-6 min (ng/ml)	4.30 ± 0.10	3.75 ± 0.12[a]	2.87 ± 0.14[a,b]	3.29 ± 0.24[a]	<0.0001
ΔCPR (ng/ml)	2.18 ± 0.07	1.93 ± 0.08	1.42 ± 0.09[a,b]	1.56 ± 0.15[a]	<0.0001

FPG: fasting plasma glucose; sCre: serum creatinine; SBP: systolic blood pressure; DBP: diastolic blood pressure.
[a] $P < 0.05$ vs. group I.
[b] $P < 0.05$ vs. group II.
[c] $P < 0.05$ vs. group III.

Table 4 – Comparison of indexes of endogenous insulin secretion between low-BMI and high-BMI subjects according to years from diagnosis.

Group (year)	I (–9.9)		II (10.0–19.9)		III (20.0–29.9)		IV (30.0–)	
BMI	<25	≥25	<25	≥25	<25	≥25	<25	≥25
Number of subjects	202	153	130	74	66	28	32	15
FCPR (ng/ml)	1.82 ± 0.06	2.52 ± 0.07[a]	1.66 ± 0.06	2.12 ± 0.12[a]	1.35 ± 0.09	1.72 ± 0.14	1.67 ± 0.15	1.85 ± 0.27
CPR-6 min (ng/ml)	3.83 ± 0.12	4.99 ± 0.15[a]	3.41 ± 0.12	4.33 ± 0.25[a]	2.70 ± 0.16	3.15 ± 0.26	3.20 ± 0.27	3.48 ± 0.50
ΔCPR (ng/ml)	2.00 ± 0.09	2.46 ± 0.11[a]	1.76 ± 0.08	2.21 ± 0.16[a]	1.38 ± 0.10	1.50 ± 0.17	1.54 ± 0.18	1.63 ± 0.27

P values were analyzed by unpaired Student *t* test.
[a] $P < 0.01$ vs. low-BMI patients.

diagnosis (–9.9 years, 10.0–19.9 years, 20.0–29.9 years, and 30.0– years) is shown in Table 3. Age, diastolic blood pressure, FCPR, CPR-6 min, and ΔCPR were significantly different among the groups. Comparison between the high-BMI and low-BMI subjects in the four groups of increasing years from diagnosis shows that FCPR, CPR-6 min, and ΔCPR were significantly increased in high-BMI subjects with years from diagnosis less than 19.9, while this was not the case when years from diagnosis was more than 20.0 (Table 4).

4. Discussion

While the present study should be interpreted carefully since it is a cross-sectional rather than a longitudinal study, we have shown that endogenous insulin secretory capacity in Japanese patients with type 2 diabetes is more closely associated with variables including years from diagnosis which reflects longer term diabetes exposure, than with variables including HbA_{1c} that reflect shorter term diabetes exposure. A decline of indexes of endogenous insulin secretion during more than several decades of diabetes was confirmed in this cross-sectional study, as was found in the longitudinal 5-year UKPDS study, although the decline became gradual. BMI is also an important independent variable to predict CPR level in type 2 diabetes.

The key role of pancreatic β-cell function in the pathogenesis of type 2 diabetes is increasingly apparent. Weyer et al. has established that impaired insulin secretion is associated with conversion from normal glucose tolerance (NGT) to impaired glucose tolerance (IGT) in a longitudinal study of Pima Indians [5]. In other studies, it has been reported that insulin secretory defect is the predominant abnormality even at an early stage of decreasing glucose tolerance [9–13]. The UKPDS findings show that pancreatic β-cell function (%β), assessed by HOMA in patients with type 2 diabetes, decreased approximately 25% in 5 years [4]. Thus, pancreatic β-cell function may continue to deteriorate as glucose intolerance progresses from NGT via IGT and non-insulin-requiring diabetes progresses to insulin-requiring diabetes [14–16].

Progressive loss of pancreatic β-cell function in patients with type 2 diabetes may be derived, at least in part, from reduced pancreatic β-cell mass, which has been found in examination of pancreatic tissue at autopsy [17–19]. One study suggests that increased apoptosis is more important in reduced β-cell mass than impaired neogenesis and proliferation in type 2 diabetes [17]. Factors in deteriorating pancreatic β-cell function during diabetic exposure including hyperglycemia, hyperlipidemia, cytokines secreted by adipocytes, immune response, and medication have been proposed based mainly on *in vitro* studies [20–22], but clinical evidence of the influence of these factors on β-cell deterioration remains to be elucidated. Assessment of insulin secretory function by HOMA in UKPDS indicated that the rates of loss of insulin secretory function were similar among groups of diet-treated, sulfonylurea-treated, and metformin-treated patients [4], which may imply that progressive β-cell deterioration occurs independent of the mode of therapy. Oxidative stress in islets of patients with type 2 diabetes, which is related to hyperglycemia and causes tissue damage, is found to be increased at autopsy [18], but clinical evidence of long-term concentration-dependent effects of hyperglycemia on β-cell deterioration is lacking.

β-Cell function increases to compensate for increased insulin resistance in subjects yet maintaining normal glucose tolerance [5]. The increase in β-cell function is brought about, at least in part, by expansion of β-cell mass, which is derived from promotion of proliferation and neogenesis and from prevention of apoptosis mediated by increased activity of growth factor signaling pathways, glucose metabolism, GLP-1 signaling, and free fatty acid metabolism and signaling [22]. Since BMI is also correlated with insulin resistance estimated by homeostasis model assessment (HOMA-IR) in Japanese patients with type 2 diabetes [23], the relationship between BMI and β-cell function is of special concern. In autopsy of subjects with normal glucose tolerance, β-cell mass is found to be greater in obese than in lean subjects [17]. These findings suggest that increased BMI may be associated with increased β-cell mass and function in subjects maintaining normal glucose tolerance. The present study also suggests that BMI is positively associated with β-cell function in patients with type 2 diabetes. This result is compatible with autopsy findings of good correlation of β-cell mass with BMI [19]. Interestingly, the time-dependent decline of CPR level was steeper in obese than in lean subjects in the present study, which is compatible with the autopsy finding that the difference in β-cell volume between non-diabetic and type 2 diabetes subjects is greater in obese than in lean subjects [17]. While a decline of β-cell function of about 5% (HOMA-β%)/year was observed in subjects with average BMI of about 30 in UKPDS, the figure might well be lower in Japanese patients whose average BMI is under 25. However, direct comparison of our measure of β-cell function using CPR in a cross-sectional study with β-cell function assessed by HOMA-β in a longitudinal UKPDS study is problematic. In the present study, larger values of endogenous insulin secretion in high-BMI subjects compared with low-BMI

subjects were observed in groups with fewer years from diagnosis, suggesting that the influence of BMI on β-cell secretory function is more prominent in disease of shorter duration. One possible explanation for this phenomenon is that the compensatory β-cell mass increase with obesity is gradually lessened by long-term diabetic exposure.

The mean of indexes of endogenous insulin secretion was higher in patients with years from diagnosis more than 30 than in patients with years from diagnosis from 20 to 29.9 (Table 3), but the difference was not significant. This result might be linked to the exclusion of patients with serum creatinine above 1.3 mg/dl, who have diabetic nephropathy with renal insufficiency most likely due to the more severe and prolonged diabetic exposure.

FCPR, but not CPR-6 min and ΔCPR, is positively correlated with serum creatinine (Fig. 4). These results indicate that in the normal range of creatinine, the serum CPR level in the fasting stable state, but not the stimulated CPR level in the dynamic state, is affected by renal function, which determines CPR clearance.

In conclusion, a linear decline in endogenous insulin secretion over more than several decades of diabetes was confirmed by this cross-sectional study. The duration of diabetes exposure and BMI are major factors in β-cell function in Japanese patients with type 2 diabetes.

Acknowledgments

This study was supported in part by Scientific Research Grants, a Grant for Leading Project for Biosimulation from the Ministry of Education, Culture, Sports, Science and Technology of Japan, and a grant from CREST of Japan Science and Technology Cooperation.

Conflict of interest

There are no conflicts of interest.

REFERENCES

[1] R.A. DeFronzo, Lilly lecture 1987. The triumvirate: beta-cell, muscle, liver. A collusion responsible for NIDDM, Diabetes 37 (1988) 667–687.
[2] H. Yki-Jarvinen, M. Kauppila, E. Kujansuu, J. Lahti, T. Marjanen, L. Niskanen, et al., Comparison of insulin regimens in patients with non-insulin-dependent diabetes mellitus, N. Engl. J. Med. 327 (1992) 1426–1433.
[3] R.C. Turner, C.A. Cull, V. Frighi, R.R. Holman, Glycemic control with diet, sulfonylurea, metformin, or insulin in patients with type 2 diabetes mellitus: progressive requirement for multiple therapies (UKPDS 49), UK Prospective Diabetes Study (UKPDS) Group, JAMA 281 (1999) 2005–2012.
[4] U.K. Prospective Diabetes Study Group, U.K. prospective diabetes study 16. Overview of 6 years' therapy of type II diabetes: a progressive disease, Diabetes 44 (1995) 1249–1258.
[5] C. Weyer, C. Bogardus, D.M. Mott, R.E. Pratley, The natural history of insulin secretory dysfunction and insulin resistance in the pathogenesis of type 2 diabetes mellitus, J. Clin. Invest. 104 (1999) 787–794.
[6] American Diabetes Association, Diagnosis and classification of diabetes mellitus, Diabetes Care 30 (Suppl. 1) (2007) S42–S47.
[7] H. Kajimuma, S. Tanabashi, K. Ishiwata, N. Kuzuya, Urinary excretion of C-peptide in relation to renal function, in: S. Baba (Ed.), Proinsulin, Insulin C-peptide, Excerpta Medica, Amsterdam, 1979, pp. 183–189.
[8] O.K. Faber, C. Binder, C-peptide response to glucagons, A test for the residual β-cell function in diabetes mellitus, Diabetes 26 (1977) 605–610.
[9] H. Yoneda, H. Ikegami, Y. Yamamoto, E. Yamato, T. Cha, Y. Kawaguchi, et al., Analysis of early-phase insulin responses in nonobese subjects with mild glucose intolerance, Diabetes Care 15 (1992) 1517–1721.
[10] E. Cerasi, R. Luft, S. Efendic, Decreased sensitivity of the pancreatic beta cells to glucose in prediabetic and diabetic subjects, a glucose dose–response study, Diabetes 21 (1972) 224–234.
[11] J. Eriksson, A. Franssila-Kallunki, A. Ekstrand, C. Saloranta, E. Widen, C. Schalin, et al., Early metabolic defects in persons at increased risk for non-insulin-dependent diabetes mellitus, N. Engl. J. Med. 321 (1989) 337–343.
[12] K. Matsumoto, S. Miyake, M. Yano, Y. Ueki, Y. Yamaguchi, S. Akazawa, et al., Glucose tolerance, insulin secretion, and insulin sensitivity in nonobese and obese Japanese subjects, Diabetes Care 20 (1997) 1562–1568.
[13] T. Kadowaki, Y. Miyake, R. Hagura, Y. Akanuma, H. Kajinuma, N. Kuzuya, et al., Risk factors for worsening to diabetes in subjects with impaired glucose tolerance, Diabetologia 26 (1984) 44–49.
[14] H.E. Lebovitz, Insulin secretagogues: old and new, Diabetes Review 7 (1999) 139–153.
[15] A. Bagust, S. Beale, Deteriorating beta-cell function in type 2 diabetes: a long-term model, QJM 96 (2003) 281–288.
[16] C.J. Rhodes, Type 2 diabetes—a matter of β-cell life and death? Science 307 (2005) 380–384.
[17] A.E. Butler, J. Janson, S. Bonner-Weir, R. Ritzel, R.A. Rizza, P.C. Butler, β-Cell deficit and increased β-cell apoptosis in humans with type 2 diabetes, Diabetes 52 (2003) 102–110.
[18] H. Sakuraba, H. Mizukami, N. Yagihashi, R. Wada, C. Hanyu, S. Yagihashi, Reduced beta-cell mass and expression of oxidative stress-related DNA damage in the islet of Japanese type II diabetic patients, Diabetologia 45 (2002) 85–96.
[19] K.H. Yoon, S.H. Ko, J.H. Cho, J.M. Lee, Y.B. Ahn, K.H. Song, et al., Selective beta-cell loss and alpha-cell expansion in patients with type 2 diabetes mellitus in Korea, J. Clin. Endocrinol. Metab. 88 (2003) 2300–2308.
[20] M.Y. Donath, P.A. Halban, Decreased beta-cell mass in diabetes: significance, mechanisms and therapeutic implications, Diabetologia 47 (2004) 581–589.
[21] D.T. Finegood, B.G. Topp, β-Cell deterioration-prospects for reversal or prevention, Diabetes Obes. Metab. 3 (Suppl. 1) (2001) S20–S27.
[22] M. Prentki, C.J. Nolan, Islet β cell failure in type 2 diabetes, J. Clin. Invest. 116 (2006) 1802–1812.
[23] A. Taniguchi, M. Fukushima, M. Saki, K. Kataoka, I. Nagata, K. Doi, et al., The role of the body mass index and triglyceride levels in identifying insulin-sensitive and insulin-resistant variants in Japanese non-insulin-dependent diabetic patients, Metabolism 49 (2000) 1001–1005.

Biochemical and Biophysical Research Communications 376 (2008) 21–25

Contents lists available at ScienceDirect

Biochemical and Biophysical Research Communications

journal homepage: www.elsevier.com/locate/ybbrc

Inhibition of GIP signaling modulates adiponectin levels under high-fat diet in mice

Rei Naitoh [a], Kazumasa Miyawaki [a], Norio Harada [a], Wataru Mizunoya [b], Kentaro Toyoda [a], Tohru Fushiki [b], Yuichiro Yamada [a,c], Yutaka Seino [a,d], Nobuya Inagaki [a,e,*]

[a] Department of Diabetes and Clinical Nutrition, Graduate School of Medicine, Kyoto University, 54 Shogoin Kawahara-cho, Sakyo-ku, Kyoto 606-8507, Japan
[b] Division of Food Science and Biotechnology, Graduate School of Agriculture, Kyoto University, Kyoto, Japan
[c] Department of Endocrinology and Diabetes and Geriatric Medicine, Akita University School of Medicine, Akita, Japan
[d] Kansai Electric Power Hospital, Osaka, Japan
[e] CREST of Japan Science and Technology Cooperation (JST), Kyoto, Japan

ARTICLE INFO

Article history:
Received 8 August 2008
Available online 22 August 2008

Keywords:
GIP
Fat oxidation
Adiponectin
PPAR

ABSTRACT

Gastric inhibitory polypeptide (GIP) is an incretin and directly promotes fat accumulation in adipocytes. Inhibition of GIP signaling prevents onset of obesity and increases fat oxidation in peripheral tissues under high-fat diet (HFD), but the mechanism is unknown. In the present study, we investigated the effects of inhibition of GIP signaling on adiponectin levels after 3 weeks of HFD by comparing wild-type (WT) mice and GIP receptor-deficient ($Gipr^{-/-}$) mice. In HFD-fed $Gipr^{-/-}$ mice, fat oxidation was significantly increased and adiponectin mRNA levels in white adipose tissue and plasma adiponectin levels were significantly increased compared to those in HFD-fed WT mice. In addition, the PPARα mRNA level was increased and the ACC mRNA level was decreased in skeletal muscle of HFD-fed $Gipr^{-/-}$ mice compared with those in HFD-fed WT mice. These results indicate that inhibition of GIP signaling increases adiponectin levels, resulting in increased fat oxidation in peripheral tissues under HFD.

Gastric inhibitory polypeptide (GIP) is a major incretin that potentiates insulin secretion in pancreatic β-cells in the presence of glucose [1,2]. GIP is released from duodenal endocrine K-cells after meal ingestion, and acts by binding the GIP receptor through increased intracellular cAMP [3]. The GIP receptor is expressed in pancreas, stomach, small intestine, heart, adrenal cortex, brain, lung, bone, vascular endothelium, and adipose tissue [4]. In addition to the insulinotropic effects on pancreatic β-cells, GIP is an obesity-promoting factor that directly leads to the accumulation of fat in adipocytes. In vitro studies show that GIP stimulates synthesis and secretion of lipoprotein lipase (LPL) in cultured preadiocytes [5], and that GIP promotes LPL activity in fat tissue [6]. It also has been shown that GIP stimulates glucose transport and increases fatty-acid synthesis in fat tissue [7]. Studies of GIP receptor-deficient mice ($Gipr^{-/-}$ mice) show that GIP also is an important factor in the promotion of obesity in vivo [8]. High-fat diet (HFD)-fed wild-type (WT) mice exhibit body weight gain and markedly increased visceral and subcutaneous fat mass and liver steatosis. By contrast, $Gipr^{-/-}$ mice fed HFD exhibit neither weight gain nor adiposity. Furthermore, measurement of the respiratory quotient reveals that fat is used as the preferred energy substrate in $Gipr^{-/-}$ mice. In addition, a study using IRS-$1^{-/-}$/$Gipr^{-/-}$ double-deficient mice demonstrated that inhibition of GIP signaling increases fatty-acid oxidation in peripheral tissues under diminished insulin signaling [9]. Thus, GIP plays a critical role in adiposity, but the mechanism of fat oxidation in peripheral tissues in the absence of GIP signaling is unclear.

Adiponectin is one of the major adipokines secreted from adipocytes, and stimulates fat oxidation in peripheral tissues. Adiponectin promotes AMPK activation and PPARα expression and stimulates fat oxidation in skeletal muscle and liver [10]. In the present study, we investigated the effects of the inhibition of GIP signaling on adiponectin levels and the stimulation of fat oxidation that averts obesity by comparing WT mice and $Gipr^{-/-}$ mice fed HFD. To clarify the early response to HFD-induced obesity, we performed the experiments on mice at 3 weeks of HFD and control-fat diet (CD).

Materials and methods

Animals. The generation of $Gipr^{-/-}$ mice (C57BL/6 background) has been described previously [11]. At 7 weeks of age, WT and $Gipr^{-/-}$ mice were fed HFD or CD for 7 weeks. HFD supplied 45% of calories as fat, 35% as carbohydrate, and 20% as protein, with energy density of 3.57 kcal/g. CD supplied 13% of calories as fat, 60% as carbohydrate, and 27% as protein, with energy density of

* Corresponding author. Address: Department of Diabetes and Clinical Nutrition, Graduate School of Medicine, Kyoto University, 54 Shogoin Kawahara-cho, Sakyo-ku, Kyoto 606-8507, Japan. Fax: +81 75 751 4244.
E-mail address: inagki@metab.kuhp.kyoto-u.ac.jp (N. Inagaki).

0006-291X/$ - see front matter © 2008 Elsevier Inc. All rights reserved.
doi:10.1016/j.bbrc.2008.08.052

3.57 kcal/g. Animal care and procedures were approved by the Animal Care Committee of Kyoto University.

Energy expenditure. Energy expenditure was evaluated by measuring respiratory quotient and oxygen consumption by indirect calorimetry every 13 min for 24 h in mice under the fed condition, as described previously [8,9,12]. Air from the room was pumped through the chamber, and expired gas was dried in a cotton thin column and subjected to gas analysis (Alco System model RL-600, Chiba, Japan). O_2 and CO_2 concentrations were measured, and oxygen consumption (VO_2), carbon dioxide exhaustion (VCO_2), respiratory quotient (RQ), and fat oxidation were calculated as described previously [12].

Computed tomography. Mice were anesthetized with pentobarbital and fixed in a chamber, and transaxially scanned using Latheta (LCT-100M) experimental animal CT system (Aloka, Tokyo, Japan). The whole body was scanned, and contiguous 1-mm slice images of the trunk were used for quantitative assessment (Latheta software, version 1.00). Weight of visceral fat mass and lean mass were quantitatively evaluated.

Measurement of plasma adiponectin levels and Western blot analysis. Blood samples were collected from the tail vein at the end of the dark phase and centrifuged (3000 rpm, 10 min, 4 °C). Levels of plasma adiponectin were measured using an adiponectin ELISA kit (Otsuka, Tokyo, Japan).

Plasma samples of HFD-fed mice were subjected to SDS–PAGE using Laemmli's method [13]. SDS–PAGE was performed under non-reducing and non-heat-denaturing conditions, as previously reported [14]. Western blot analysis was performed using anti-mouse adiponectin antibody. Densities of corresponding bands were quantified by NIH-Image.

Isolation of total RNA and quantitative RT-PCR. Total RNA was isolated from muscle and white adipose tissue (epididymal fat pad, (WAT)) using Trizol (Invitrogen, Grand Island, NY). mRNA levels were measured by real-time quantitative RT-PCR using ABI PRISM 7000 Sequence Detection System (Applied Biosystems, Foster City, CA). mRNA levels were corrected for GAPDH (Applied Biosystems) mRNA level. Sequences of PPARα primers were 5′-CGACCTGAAAG ATTCGGAAA-3′ and 5′-CCTCTGCCTCTTTGTCTTC-3′; sequences of ACC primers were 5′-CCTCCGAGGAACCCTCTGT-3′ and 5′-CGGCTGT CCAGTTGGTTTG-3′; sequences of adiponectin primers were 5′-G GAACTTGTGCAGGTTGGAT-3′ and 5′-GCTTCTCCAGGCTCTCCTTT-3′; and sequences of PPARγ primers were 5′-TGTCGGTTTCAGAAGT GCCTT-3′ and 5′-GCTCGCAGATCAGCAGACTCT-3′.

Statistical analysis. Data are expressed as means ± SE. Statistical analysis was performed by ANOVA and unpaired student's test. P values <0.05 were considered significant.

Results

Body weight and fat mass in HFD-fed Gipr$^{-/-}$ mice

WT mice exhibited significant weight gain after 3 weeks of HFD feeding (Fig. 1A). By contrast, body weight of HFD-fed Gipr$^{-/-}$ mice was not increased compared with that of CD-fed Gipr$^{-/-}$ mice after 3 weeks of study (Fig. 1B). The lesser body weight of Gipr$^{-/-}$ mice continued through 7 weeks of HFD feeding.

At the early stage of 3 weeks of HFD feeding, CT analysis was performed to estimate visceral fat mass in WT and Gipr$^{-/-}$ mice. There was no significant difference in visceral fat mass between WT and Gipr$^{-/-}$ mice under CD feeding. Visceral fat mass of HFD-fed WT and Gipr$^{-/-}$ mice were significantly increased compared with those of CD-fed WT and Gipr$^{-/-}$ mice by 100% and 52%, respectively. In HFD-fed mice, visceral fat mass of WT mice was significantly increased compared with that of Gipr$^{-/-}$ mice (Fig. 1C and D). There was no difference in lean body mass (data not shown). There also was no difference in food intake between WT and Gipr$^{-/-}$ mice (data not shown).

Fat consumption in HFD-fed Gipr$^{-/-}$ mice

To evaluate energy consumption in the early stage of HFD feeding, respiratory quotient and oxygen consumption were measured

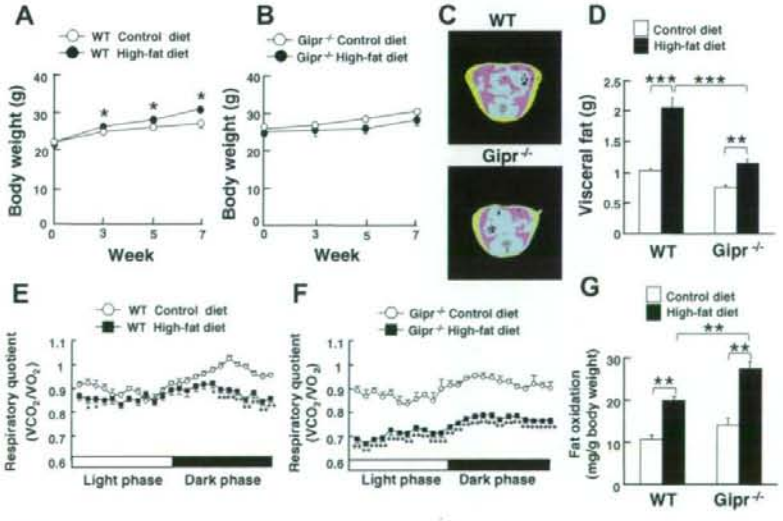

Fig. 1. Body weight in WT mice (A) and Gipr$^{-/-}$ mice (B) during 7 weeks on CD (open circles) and HFD (filled circles). (C) CT-based body composition analysis. WT mice and Gipr$^{-/-}$ mice at 3 weeks on HFD feeding. Representative CT images were taken at the same slice level. Pink, yellow, and blue areas represent visceral fat, subcutaneous fat, and lean mass. (D) Visceral fat accumulation in WT mice and Gipr$^{-/-}$ mice at 3 weeks on CD (open bars) and HFD (filled bars). Respiratory quotient in WT mice (E) and Gipr$^{-/-}$ mice (F) at 3 weeks on CD (open circles) and HFD (filled square). (G) Calculated fat oxidation in WT mice and Gipr$^{-/-}$ mice at 3 weeks on CD (open bars) and HFD (filled bars). n = 5–12. Values are means ± SE. $^{*}P < 0.05$, $^{**}P < 0.01$, $^{***}P < 0.005$. (For interpretation of the references to color in this figure legend, the reader is referred to the web version of this paper.)

by indirect calorimetry. HFD-fed WT mice exhibited a significant reduction of respiratory quotient only in part of the dark phase compared with CD-fed WT mice (Fig. 1E). By contrast, HFD-fed Gipr$^{-/-}$ mice exhibited a significant reduction of respiratory quotient throughout the day compared with CD-fed Gipr$^{-/-}$ mice (Fig. 1F). At 3 weeks of HFD feeding, calculated fat oxidation was significantly increased in Gipr$^{-/-}$ mice compared with that in WT mice (Fig. 1G). These results indicate that Gipr$^{-/-}$ mice use fat as preferred energy substrate in the early stage of HFD feeding.

Adiponectin levels of Gipr$^{-/-}$ mice in the early stage of HFD feeding

We examined mRNA expression level of adiponectin in white adipose tissue (WAT) and plasma adiponectin levels in Gipr$^{-/-}$ mice. mRNA expression of adiponectin in WAT and plasma adiponectin levels were significantly increased in HFD-fed Gipr$^{-/-}$ mice compared with those in HFD-fed WT mice (Fig. 2A and B). In addition, in Gipr$^{-/-}$ mice, mRNA expression level of adiponectin in WAT and plasma adiponectin levels were significantly increased in HFD-fed mice compared with those in CD-fed mice, although HFD feeding decreased mRNA expression of adiponectin and plasma adiponectin levels in WT mice (Fig. 2A and B).

To determine qualitative differences in adiponectin, we performed Western blot analysis. Levels of middle molecular weight (MMW) and low molecular weight (LMW) multimers of adiponectin were significantly higher in HFD-fed Gipr$^{-/-}$ mice compared to those in HFD-fed WT mice (Fig. 2C and Table 1). There were no significant differences in high molecular weight multimers (HMW) of adiponectin between HFD-fed WT and Gipr$^{-/-}$ mice.

As PPARγ (peroxisome proliferator-activated receptor-γ) is known to be involved in the regulation of adiponectin, we examined mRNA expression levels of PPARγ in WAT. While HFD-fed WT mice showed a tendency to decreased mRNA expression of PPARγ, the mRNA expression level of PPARγ was significantly increased in HFD-fed Gipr$^{-/-}$ mice compared with that in HFD-fed WT mice (Fig. 2D). These results suggest that inhibition of GIP signaling modulates adiponectin levels through PPARγ.

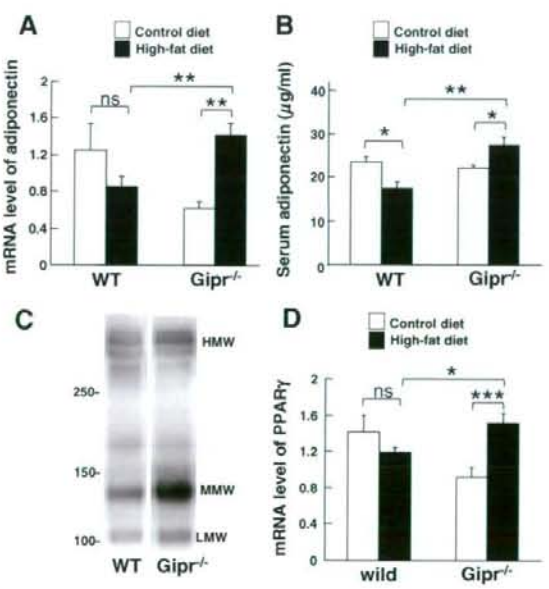

Fig. 2. mRNA expression level of adiponectin in WAT (A) and plasma adiponectin level (B) at 3 weeks on CD (open bars) and HFD (filled bars). $n = 7$–8 mice/group. Values are means ± SE. $^{*}P < 0.05$, $^{**}P < 0.01$. (C) Non-reducing and non-heat-denaturing SDS-PAGE of adiponectin in WT mice and Gipr$^{-/-}$ mice at 3 weeks on HFD. (D) mRNA expression level of PPARγ in WAT at 3 weeks on CD (open bars) and HFD (filled bars). $n = 4$–7. Values are means ± SE. $^{*}P < 0.05$, $^{***}P < 0.005$, ns, not significant.

Table 1
Difference in multimer formation of adiponectin in WT mice and Gipr$^{-/-}$ mice at 3 weeks on high-fat diet

	WT	Gipr$^{-/-}$
HMW	100 ± 22.0	131.9 ± 17.8
MMW	100 ± 9.1	154.3 ± 5.9*
LMW	100 ± 13	163.4 ± 15.3*

Values for Gipr$^{-/-}$ mice represent relative density (%) regarding average value for WT mice as 100. $n = 5$. Values are means ± SE.
* $P < 0.05$ vs. WT mice.

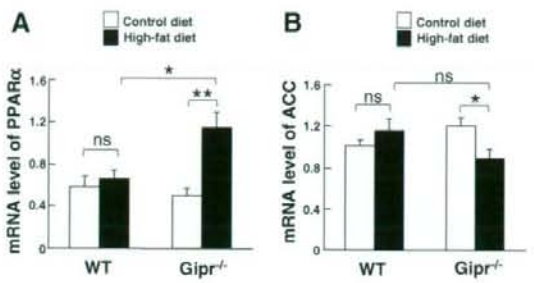

Fig. 3. mRNA expression level of PPARα (A) and ACC (B) in skeletal muscle at 3 weeks on CD (open bars) and HFD (filled bars). $n = 5$–7. Values are means ± SE. $^{*}P < 0.05$, $^{**}P < 0.01$. ns, not significant.

Expression levels of PPARα and ACC mRNAs in skeletal muscle of Gipr$^{-/-}$ mice at the early stage of HFD feeding

To determine the effects of adiponectin on peripheral tissues in the absence of GIP signaling, mRNA expression levels of PPARα (peroxisome proliferator-activated receptor-α) and ACC (acetyl-CoA carboxylase) in skeletal muscle and liver were examined. mRNA expression level of PPARα mRNA was significantly increased in HFD-fed Gipr$^{-/-}$ mice compared with that in CD-fed Gipr$^{-/-}$ mice in skeletal muscle (Fig. 3A). Although there was no significant difference in phosphorylation of AMPK (AMP-activated protein kinase) between HFD-fed WT and Gipr$^{-/-}$ mice by western blot analysis (data not shown), mRNA expression level of ACC, which is inactivated by AMPK, was significantly reduced in muscle of HFD-fed Gipr$^{-/-}$ mice compared with that in CD-fed Gipr$^{-/-}$ mice (Fig. 3B). These results indicate that fat oxidation is increased in skeletal muscle of Gipr$^{-/-}$ mice in the early stage of HFD feeding. We also examined mRNA expression levels of PPARα and ACC in liver, but no significant differences were found among the groups of mice (data not shown).

Discussion

In this study, we investigated the effects of GIP inhibition on fat oxidation in the early stage (3 weeks) of HFD feeding, and found that inhibition of GIP signaling increases the level of adiponectin, which promotes fat oxidation in peripheral tissues.

The GIP receptor is expressed in adipocytes as well as in pancreatic β-cells, and GIP signaling directly promotes energy accumulation into adipocytes. Previously, Gipr$^{-/-}$ mice were shown to exhibit resistance to high-fat-induced obesity, and to use fat as the preferred energy substrate [8]. In that study, mice were fed

HFD for a long period of from 7 to 50 weeks of age. In the present study, we investigated HFD-fed mice in the short, early period from 7 to 10 weeks of age, and found Gipr$^{-/-}$ mice to be resistant to obesity as well as to accumulation of visceral fat, and that fat oxidation was significantly increased, demonstrating that GIP plays a critical role in promoting obesity even at 3 weeks on HFD feeding.

Leptin and adiponectin are major adipokines that activate fat oxidation for body weight control. They affect AMPK activation and stimulate fat oxidation in skeletal muscle and liver [10,15]. It has been reported that inhibition of GIP signaling decreases body weight even in leptin-deficient ob/ob mice [8], indicating that factors other than leptin increase fat oxidation under conditions of inhibited GIP signaling. Leptin suppresses food intake through the central nervous system, and there were no differences in food intake between WT and Gipr$^{-/-}$ mice in CD-fed and HFD-fed mice in the present study. Thus, we focused on adiponectin, and hypothesized that inhibition of GIP signaling modulates adiponectin levels and affects on fat oxidation in peripheral tissues. The mRNA expression level of adiponectin in adipocytes and adiponectin concentrations in plasma are reduced in obese and insulin-resistant states which increases visceral fat mass [16,17]. In the present study, mRNA expression level of adiponectin in WAT and plasma adiponectin levels were found to be decreased and visceral fat mass was increased in HFD-fed WT mice compared with CD-fed WT mice. The mRNA expression and plasma levels of adiponectin were significantly increased in HFD-fed Gipr$^{-/-}$ mice compared with those in CD-fed Gipr$^{-/-}$ mice, although visceral fat mass of HFD-fed Gipr$^{-/-}$ mice was significantly increased compared with that of CD-fed Gipr$^{-/-}$ mice. These results suggest that GIP may reduce adiponectin levels in adipocytes. It has been previously reported that Gipr$^{-/-}$ mice show no difference in plasma adiponectin levels between CD-fed and HFD-fed mice after a long period of 20 weeks, when obesity is established [18]. On the other hand, we measured adiponectin levels of mice fed HFD for a short period of 3 weeks, and demonstrate that inhibition GIP signaling modulates adiponectin even in the very early stage when obesity first begins to appear in WT mice.

While skeletal muscle and liver are the major sites of body fat oxidation, the GIP receptor is not expressed in these tissues. PPARα and AMPK are the most important molecules in the control of fat oxidation in muscle and liver. Adiponectin increases expression levels of PPARα and induces phosphorylation of AMPK [16,19]. AMPK activated by adiponectin suppresses ACC activity, which catalyses the formation of malonyl-CoA and stimulates fat oxidation [20]. We found that the mRNA expression level of PPARα was significantly increased and that of ACC was significantly reduced in skeletal muscle of HFD-fed Gipr$^{-/-}$ mice compared to those in CD-fed Gipr$^{-/-}$ mice. These results indicate that fat oxidation is increased in skeletal muscle of Gipr$^{-/-}$ mice in the early stage of HFD feeding, but there was no significant difference in liver. Adiponectin has three forms: trimers (low molecular weight, LMW), hexamers (middle molecular weight, MMW), and multimers (high molecular weight, HMW), and differing tissue-specific effects of these forms on AMPK phosphorylation have been reported [21]. Only trimers activate AMPK in muscle; hexamers and the high molecular isoform do not [22]. It also has been reported that trimers are the most potent isoform in skeletal muscle [19,23]. The trimer isoform of adiponectin was found in the present study to be significantly increased in HFD-fed Gipr$^{-/-}$ mice. This finding may explain the difference of PPARα and ACC expression between skeletal muscle and liver in HFD-fed Gipr$^{-/-}$ mice.

In conclusion, we show that inhibition of GIP signaling upregulates the adiponectin level and increases fat oxidation in skeletal muscle. These findings suggest that the influence of GIP on adiposity is, at least in part, mediated by modulation of adiponectin expression in adipocytes in the early stage of HFD feeding.

Acknowledgments

We thank Drs. Takashi Kadowaki and Naoto Kubota (Department of Diabetes and Metabolic Disease, Tokyo University Graduate School of Medicine) for providing anti-mouse adiponectin antibody and for their valuable suggestion.

We also thank Drs. Katsushi Tsukiyama, Rie Watanabe, Heying Zhou, Chizumi Yamada, and Yukiko Kawasaki for their technical help and for their valuable comments.

This study was supported by Scientific Research Grants from the Ministry of Education, Culture, Sports, Science, and Technology, Japan, and from the Ministry of Health, Labor, and Welfare, Japan.

References

[1] P. Schauder, J. Brown, H. Frerichs, W. Creutzfeldt, Gastric inhibitory polypeptide: effect on glucose-induced insulin release from isolated rat pancreatic islets in vitro, Diabetologia 11 (1975) 483–484.
[2] J. Dupre, S. Ross, D. Watson, J. Brown, Stimulation of insulin secretion by gastric inhibitory polypeptide in man, J. Clin. Endocrinol. Metab. 37 (1973) 826–828.
[3] Y. Yamada, K. Miyawaki, K. Tsukiyama, N. Harada, C. Yamada, Y. Seino, Pancreatic and extrapancreatic effects of gastric inhibitory polypeptide, Diabetes 55 (Suppl. 2) (2006) S86–S91.
[4] T.B. Usdin, E. Mezey, D.C. Button, M.J. Brownstein, T.I. Bonner, Gastric inhibitory polypeptide receptor, a member of the secretin-vasoactive intestinal peptide receptor family, is widely distributed in peripheral organs and the brain, Endocrinology 133 (1993) 2861–2870.
[5] R.H. Eckel, W.Y. Fujimoto, J.D. Brunzell, Gastric inhibitory polypeptide enhanced lipoprotein lipase activity in cultured preadipocytes, Diabetes 28 (1979) 1141–1142.
[6] J. Knapper, S. Puddicombe, L. Morgan, J. Fletcher, Investigations into the actions of glucose-dependent insulinotropic polypeptide and glucagon-like peptide-1(7-36)amide on lipoprotein lipase activity in explants of rat adipose tissue, J. Nutr. 125 (1995) 183–188.
[7] H. Hauner, G. Glatting, D. Kaminska, E. Pfeiffer, Effects of gastric inhibitory polypeptide on glucose and lipid metabolism of isolated rat adipocytes, Ann. Nutr. Metab. 32 (1988) 282–288.
[8] K. Miyawaki, Y. Yamada, N. Ban, Y. Ihara, K. Tsukiyama, H. Zhou, S. Fujimoto, A. Oku, K. Tsuda, S. Toyokuni, H. Hiai, W. Mizunoya, T. Fushiki, J. Holst, M. Makino, A. Tashita, Y. Kobara, Y. Tsubamoto, T. Jinnouchi, T. Jomori, Y. Seino, Inhibition of gastric inhibitory polypeptide signaling prevents obesity, Nat. Med. 8 (2002) 738–742.
[9] H. Zhou, Y. Yamada, K. Tsukiyama, K. Miyawaki, M. Hosokawa, K. Nagashima, K. Toyoda, R. Naitoh, W. Mizunoya, T. Fushiki, T. Kadowaki, Y. Seino, Gastric inhibitory polypeptide modulates adiposity and fat oxidation under diminished insulin action, Biochem. Biophys. Res. Commun. 335 (2005) 937–942.
[10] T. Kadowaki, T. Yamauchi, Adiponectin and adiponectin receptors, Endocr. Rev. 26 (2005) 439–451.
[11] K. Miyawaki, Y. Yamada, H. Yano, H. Niwa, N. Ban, Y. Ihara, A. Kubota, S. Fujimoto, M. Kajikawa, A. Kuroe, K. Tsuda, H. Hashimoto, T. Yamashita, T. Jomori, F. Tashiro, J. Miyazaki, Y. Seino, Glucose intolerance caused by a defect in the entero-insular axis: a study in gastric inhibitory polypeptide receptor knockout mice, Proc. Natl. Acad. Sci. USA 96 (1999) 14843–14847.
[12] K. Ishihara, S. Oyaizu, K. Onuki, K. Lim, T. Fushiki, Chronic (−)-hydroxycitrate administration spares carbohydrate utilization and promotes lipid oxidation during exercise in mice, J. Nutr. 130 (2000) 2990–2995.
[13] U.K. Laemmli, Cleavage of structural proteins during the assembly of the head of bacteriophage T4, Nature 227 (1970) 680–685.
[14] H. Waki, T. Yamauchi, J. Kamon, Y. Ito, S. Uchida, S. Kita, K. Hara, Y. Hada, F. Vasseur, P. Froguel, S. Kimura, R. Nagai, T. Kadowaki, Impaired multimerization of human adiponectin mutants associated with diabetes. Molecular structure and multimer formation of adiponectin, J. Biol. Chem. 278 (2003) 40352–40363.
[15] Y. Minokoshi, Y. Kim, O. Peroni, L. Fryer, C. Müller, D. Carling, B. Kahn, Leptin stimulates fatty-acid oxidation by activating AMP-activated protein kinase, Nature 415 (2002) 339–343.
[16] T. Yamauchi, J. Kamon, H. Waki, Y. Imai, N. Shimozawa, K. Hioki, S. Uchida, Y. Ito, K. Takakuwa, J. Matsui, M. Takata, K. Eto, Y. Terauchi, K. Komeda, M. Tsunoda, K. Murakami, Y. Ohnishi, T. Naitoh, K. Yamamura, Y. Ueyama, P. Froguel, S. Kimura, R. Nagai, T. Kadowaki, Globular adiponectin protected ob/ob mice from diabetes and ApoE-deficient mice from atherosclerosis, J. Biol. Chem. 278 (2003) 2461–2468.
[17] C. Weyer, T. Funahashi, S. Tanaka, K. Hotta, Y. Matsuzawa, R. Pratley, P. Tataranni, Hypoadiponectinemia in obesity and type 2 diabetes: close association with insulin resistance and hyperinsulinemia, J. Clin. Endocrinol. Metab. 86 (2001) 1930–1935.
[18] T. Hansotia, A. Maida, G. Flock, Y. Yamada, K. Tsukiyama, Y. Seino, D.J. Drucker, Extrapancreatic incretin receptors modulate glucose homeostasis, body weight, and energy expenditure, J Clin Invest 117 (2007) 143–152.
[19] T. Yamauchi, J. Kamon, H. Waki, Y. Terauchi, N. Kubota, K. Hara, Y. Mori, T. Ide, K. Murakami, N. Tsuboyama-Kasaoka, O. Ezaki, Y. Akanuma, O. Gavrilova, C.

Vinson, M. Reitman, H. Kagechika, K. Shudo, M. Yoda, Y. Nakano, K. Tobe, R. Nagai, S. Kimura, M. Tomita, P. Froguel, T. Kadowaki, The fat-derived hormone adiponectin reverses insulin resistance associated with both lipoatrophy and obesity, Nat. Med. 7 (2001) 941–946.
[20] B. Kiens, Skeletal muscle lipid metabolism in exercise and insulin resistance, Physiol. Rev. 86 (2006) 205–243.
[21] M. Barnea, A. Shamay, A. Stark, Z. Madar, A high-fat diet has a tissue-specific effect on adiponectin and related enzyme expression, Obesity (Silver Spring) 14 (2006) 2145–2153.
[22] T. Tsao, E. Tomas, H. Murrey, C. Hug, D. Lee, N. Ruderman, J. Heuser, H. Lodish, Role of disulfide bonds in Acrp30/adiponectin structure and signaling specificity. Different oligomers activate different signal transduction pathways, J. Biol. Chem. 278 (2003) 50810–50817.
[23] J. Fruebis, T. Tsao, S. Javorschi, D. Ebbets-Reed, M. Erickson, F. Yen, B. Bihain, H. Lodish, Proteolytic cleavage product of 30-kDa adipocyte complement-related protein increases fatty acid oxidation in muscle and causes weight loss in mice, Proc. Natl. Acad. Sci. USA 98 (2001) 2005–2010.

Am J Physiol Endocrinol Metab 294: E61–E68, 2008.
First published October 30, 2007; doi:10.1152/ajpendo.00358.2007.

A novel GIP receptor splice variant influences GIP sensitivity of pancreatic β-cells in obese mice

Norio Harada,[1] Yuichiro Yamada,[1] Katsushi Tsukiyama,[1] Chizumi Yamada,[1] Yasuhiko Nakamura,[1] Eri Mukai,[1,2] Akihiro Hamasaki,[1] Xibao Liu,[1] Kentaro Toyoda,[1] Yutaka Seino,[1,3] and Nobuya Inagaki[1,4]

[1]*Department of Diabetes and Clinical Nutrition, Kyoto University Graduate School of Medicine, Kyoto;* [2]*Japan Association for the Advancement of Medical Equipment, Tokyo;* [3]*Kansai Electric Power Hospital, Osaka; and* [4]*Core Research for Evolutional Science and Technology of Japan Science and Technology, Kyoto, Japan*

Submitted 11 June 2007; accepted in final form 11 October 2007

Harada N, Yamada Y, Tsukiyama K, Yamada C, Nakamura Y, Mukai E, Hamasaki A, Liu X, Toyoda K, Seino Y, Inagaki N. A novel GIP receptor splice variant influences GIP sensitivity of pancreatic β-cells in obese mice. *Am J Physiol Endocrinol Metab* 294: E61–E68, 2008. First published October 30, 2007; doi:10.1152/ajpendo.00358.2007.— Gastric inhibitory polypeptide (GIP) is an incretin that potentiates insulin secretion from pancreatic β-cells by binding to GIP receptor (GIPR) and subsequently increasing the level of intracellular adenosine 3′,5′-cyclic monophosphate (cAMP). We have identified a novel GIPR splice variant in mouse β-cells that retains intron 8, resulting in a COOH-terminal truncated form (truncated GIPR). This isoform was coexpressed with full-length GIPR (wild-type GIPR) in normal GIPR-expressing tissues. In an experiment using cells transfected with both GIPRs, truncated GIPR did not lead to cAMP production induced by GIP but inhibited GIP-induced cAMP production through wild-type GIPR ($n = 3$–4, $P < 0.05$). Wild-type GIPR was normally located on the cell surface, but its expression was decreased in the presence of truncated GIPR, suggesting a dominant negative effect of truncated GIPR against wild-type GIPR. The functional relevance of truncated GIPR in vivo was investigated. In high-fat diet-fed obese mice (HFD mice), blood glucose levels were maintained by compensatory increased insulin secretion ($n = 8$, $P < 0.05$), and cAMP production ($n = 6$, $P < 0.01$) and insulin secretion ($n = 10$, $P < 0.05$) induced by GIP were significantly increased in isolated islets, suggesting hypersensitivity of the GIPR. Total GIPR mRNA expression was not increased in the islets of HFD mice, but the expression ratio of truncated GIPR to total GIPR was reduced by 32% compared with that of control mice ($n = 6$, $P < 0.05$). These results indicate that a relative reduction of truncated GIPR expression may be involved in hypersensitivity of GIPR and hyperinsulinemia in diet-induced obese mice.

gastric inhibitory polypeptide; gastric inhibitory polypeptide receptor; alternative splicing; dominant negative effect; obesity

OBESITY LEADS TO INSULIN RESISTANCE, characterized by fasting hyperinsulinemia and excessive insulin secretion after meal ingestion in the attempt to maintain euglycemia (25). Obesity is an important risk factor in progression to type 2 diabetes mellitus (14) and also in cardiovascular disease (16), and reduction of obesity can normalize hyperinsulinemia and impede the progression of diabetes and arteriosclerosis.

Incretins are a group of peptide hormones released from the gastrointestinal tract into the circulation in response to meal ingestion that potentiate glucose-stimulated insulin secretion and include gastric inhibitory polypeptide (GIP), also called glucose-dependent insulinotropic polypeptide (24). GIP is secreted from the K cells of the duodenum and proximal jejunum upon meal ingestion and binds to the GIP receptor (GIPR) on the surface of pancreatic β-cells, adipose tissues, and osteoblasts to stimulate insulin secretion (21), fat accumulation (20), and bone formation (30) by increasing the level of intracellular adenosine 3′,5′-cyclic monophosphate (cAMP).

Previously, we found that GIPR-deficient mice exhibit insufficient compensatory insulin secretion upon high-fat loading (21), indicating that GIP plays a critical role in maintaining the blood glucose level by inducing hypersecretion of insulin in diet-induced obesity. Increased GIP signaling in obesity might be due to hypersecretion of GIP from K cells or hypersensitivity of GIPR to GIP at the β-cells. An increased blood GIP level in obesity has been reported in some studies (3, 6) but is controversial (27, 28), and altered GIPR sensitivity in obesity has not been investigated.

GIPR is the G protein-coupled receptor (GPCR) that belongs to the secretin-vasoactive intestinal peptide receptor family (31, 33). The gene encoding the human GIPR contains 14 exons (33); the rat and mouse GIPR-encoding genes contain 15 exons (2, 21). Alternative splicing is a frequent occurrence in the transcriptome in higher eukaryotic cells and can alter the structure of the encoded protein and dramatically increase the efficiency of the proteome in regulating cell function. In the present study, we report a novel splice variant GIPR expressed in mouse pancreatic β-cells and the investigation of its functional significance in hypersensitivity of GIPR in high-fat diet-induced obese mice.

MATERIALS AND METHODS

Animals. Male C57BL/6 mice (7 wk old) were obtained from Shimizu (Kyoto, Japan). The animals were fed control fat chow (CFD; 10% fat, 20% protein, and 70% carbohydrate by energy) or high-fat chow (HFD; 45% fat, 20% protein, and 35% carbohydrate by energy) for 10 wk. The energy density of both diets was 3.57 kcal/g. After a 16-h fast, oral glucose tolerance tests (OGTTs) (2 g/kg body wt) were performed in CFD and HFD mice. Blood glucose and plasma insulin levels were measured in samples taken at the indicated times. Blood glucose levels were determined by the glucose oxidase method. Plasma insulin levels were determined using enzyme immunoassay (Shibayagi, Gumma, Japan). Animal care and procedures were approved by the Animal Care Committee of Kyoto University.

Address for reprint requests and other correspondence: Y. Yamada, Dept. of Internal Medicine, Div. of Endocrinology, Diabetes, and Geriatric Medicine, Akita University School of Medicine, 1-1-1, Hondo, Akita 010-8543, Japan (e-mail: yamada@gipc.akita-u.ac.jp).

The costs of publication of this article were defrayed in part by the payment of page charges. The article must therefore be hereby marked "*advertisement*" in accordance with 18 U.S.C. Section 1734 solely to indicate this fact.

Isolation and measurement of GIPR mRNA. Total RNA was extracted from tissues (pancreatic islets, proximal jejunum, and adipose tissues) of C57/BL6 mice and Wistar rats (Shimizu) and mouse pancreatic β-cell line MIN6 cells with RNeasy mini kit (Qiagen, Valencia, CA). Islets were isolated by collagenase digestion (29). The extracted RNA was treated with DNase (Qiagen), and the cDNA was prepared by reverse transcription (Superscript II; Invitrogen, Grand Island, NY) with an oligo(dT) primer. To detect mouse full-length GIPR, COOH-terminal and NH_2-terminal primers of GIPR were designed as follows: forward, 5′-CTTTTCAAGGATGCCCCTGCGGTTGC-3′; reverse, 5′-CCTTTACCTAGCAGTAACTTTTCCAAGA-3′. The cDNA was amplified through 35 cycles with denaturation at 96°C for 15 s, annealing at 60°C for 30 s, and extension at 72°C for 2 min. To clearly detect splice variants of GIPR, a pair of GIPR primers was designed as follows: mouse GIPR forward, 5′-CTGCCTGCCGCACGGCCCAGAT-3′; reverse, 5′-CAAATGGCTTTGACTTCGTTG-3′; rat GIPR forward, 5′-CTGCCTGCCGCACAGCCCAGAT-3′; reverse, 5′- CAAATGGCTTTGACTTCGTTG -3′. The cDNA was amplified through 40 cycles with denaturation at 95°C for 15 s, annealing at 55°C for 15 s, and extension at 72°C for 30 s. The PCR products were fractioned on 2% agarose gels. Negative controls of cDNAs of tissues were prepared in the absence of reverse transcriptase at the reverse transcription step.

GIPR mRNA levels in the islets were measured by quantitative RT-PCR using ABI PRISM 7000 Sequence Detection System (Applied Biosystems, Foster City, CA). The mouse sequences of forward and reverse primers to evaluate total GIPR expression were 5′-CCTCCACTGGGTCCCTACAC-3′ and 5′-GATAAACACCCTCCACCAGTAG-3′, respectively, whereas the sequences of forward and reverse primers to evaluate truncated GIPR expression were 5′-CCTACCCCGTGGAACCAG-3′ and 5′-GTGGTGGGGAGCCAAGAT-3′, respectively. SYBR Green PCR Master Mix (Applied Biosystems) was prepared for PCR run. The thermal cycling conditions were denaturation at 95°C for 10 min followed by 50 cycles at 95°C for 15 s and 60°C for 1 min. Total GIPR mRNA levels were corrected for GAPDH (Applied Biosystems) mRNA levels.

Plasmid construction. The cDNA fragments of mouse wild-type GIPR, truncated GIPR, and $G_s\alpha$ protein were obtained from mouse (C57BL/6) islets by RT-PCR. The cDNA fragment of wild-type GIPR was cloned into pCMV-6c vector and pFLAG-CMV-5b vector (wild-type GIPR-FLAG; Sigma, St. Louis, MO). The cDNA fragment of truncated GIPR was cloned into pCMV-6c vector and pAcGFP-N1 vector (truncated GIPR-GFP; Takara, Tokyo, Japan). The two GIPR constructs were FLAG- or green fluorescent protein (GFP)-tagged at the COOH terminus. The cDNA fragment of mouse $G_s\alpha$ protein was cloned into pCMV-6c vector.

Cell culture and transfection. COS-7 cells were seeded in 10-cm dishes and cultured in Dulbecco's modified Eagle's medium supplemented with 10% fetal bovine serum. Expression plasmids of wild-type GIPR, truncated GIPR, wild-type GIPR-FLAG, and truncated GIPR-GFP were transfected into COS-7 cells using FuGENE 6 transfection reagent (Roche, Basel, Switzerland). Plasmid (5 μg/well) was diluted into serum-free medium, and FuGENE 6 reagent was added and incubated at room temperature for 30 min. After incubation, the mixture was added to COS-7 cells.

Measurement of intracellular cAMP level in GIPR-expressing COS-7 cells. COS-7 cells were transfected with the wild-type GIPR expression plasmid and the truncated GIPR expression plasmid using the amounts indicated in figure legends, passaged after 24 h into 12-well plates (1×10^5 cells/well), and cultured for an additional 48 h. The cells were washed twice with phosphate-buffered saline (PBS), and the reaction was started in 0.5 ml of Krebs-Ringer bicarbonate buffer (KRBB) containing 0.1 mM 3-isobutyl-1-methylxanthine (IBMX) with various concentrations of mouse GIP (provided by Sanwakagaku Kenkyusho, Mie, Japan) and then incubated at 37°C for 30 min. Incubation buffers were removed and the cells lysed by addition of 0.1 M HCl (0.5 ml/well) to each well (15). Plates were incubated at room temperature for 15 min with gentle rotation. The samples were centrifuged for 10 min at 600 *g*. cAMP levels were measured by enzyme immunoassay (cAMP low pH EIA kit; R&D Systems, Minneapolis, MN). Data were expressed as the increment with GIP treatment from basal cAMP levels.

Fluorescence microscopy. Immunofluorescence staining was performed using COS-7 cells either transfected with the wild-type GIPR-FLAG expression plasmid (2 μg) or the truncated GIPR-GFP expression plasmid (2 μg) or cotransfected with the two plasmids (1 μg each) with $G_s\alpha$ protein expression plasmid (2 μg). We used $G_s\alpha$ protein expression plasmid for structural stability of wild-type GIPR on plasma membrane (11). The cells were cultured on coverslips for 72 h, washed twice with PBS, and treated with acetone-methanol (1:1) for 4 min. After being washed sequentially with PBS containing 1% bovine serum albumin (BSA), the cells were incubated at room temperature for 24 h with anti-GFP monoclonal mouse antibody (Sigma) and anti-FLAG polyclonal rabbit antibody (Sigma) or anti-calnexin rabbit polyclonal antibody (Stressgen, San Diego, CA) in PBS containing 1% BSA. After being washed three times with PBS, the cells were immunostained at room temperature for 1 h using Cy3-conjugated anti-rabbit IgG (Sigma) or Alexa fluor 488 anti-mouse IgG (Molecular Probes, Eugene, OR) (23). Fluorescent images were analyzed using a confocal laser microscope LSM510 Meta (Carl Zeiss, Heidelberg, Germany).

Binding assay. Binding assay was performed using COS-7 cells either transfected with the wild-type GIPR expression plasmid (1 μg) or the truncated GIPR expression plasmid (1 μg) or cotransfected with the two plasmids (1 μg each) (total amount of plasmid DNA used for transfection was adjusted to 5 μg by adding pCMV-6c vector). After 72 h of incubation the cells were washed twice with PBS, and the collected cells were incubated with ^{125}I-labeled GIP (50,000 counts/min; Amersham Biosciences, Piscataway, NJ) in 1 ml of buffer containing 50 mM Tris (pH 7.4), 0.2 mM sucrose, 5 mM $MgCl_2$, and 1 mg/ml bacitracin at 22°C for 1 h in the absence or presence of 10^{-6} M nonradioactive GIP. Samples were filtered through Whatman GF/C filters (24 mm) and rapidly washed three times with ice-cold PBS. The radioactivity of the filters was measured in a γ-counter (22). Competitive binding assay was also performed using COS-7 cells transfected with the wild-type GIPR expression plasmid (1 μg) or cotransfected with the two plasmids (1 μg each). Various concentrations of nonradioactive GIP, ranging from 10^{-12} to 10^{-6} M, were used as competitors. Specific binding of radioactive GIP was calculated by subtracting binding of radioactive GIP in the presence of nonradioactive GIP. Protein content was measured by Bradford method. Data were expressed as specific binding to each of the GIPR-expressing cells after subtraction of the specific binding to cells transfected with pCMV-6c vector.

Immunoprecipitation and Western blot analysis. We performed Western blot analysis using COS-7 cells either transfected with the wild-type GIPR-FLAG expression plasmid (2 μg) or the truncated GIPR-GFP expression plasmid (2 μg) or cotransfected with the two plasmids (1 μg each). After 72 h of incubation, the collected cells were washed twice with PBS containing protease inhibitor (Complete; Roche) and suspended in 1 ml of PBS containing protease inhibitor. The cells were homogenized and centrifuged at 800 *g* for 5 min. The supernatant was centrifuged at 10,000 *g* for 10 min. The supernatant was further centrifuged at 100,000 *g* for 30 min to separate the endoplasmic reticulum (ER)-enriched fraction and the supernatant. The ER-enriched fraction was solubilized in 1 ml of PBS containing protease inhibitor and 2% Triton X-100 on ice for 15 min and centrifuged at 15,000 *g* for 10 min. The supernatant was incubated at 4°C for 2 h with mixing for immunoprecipitation using anti-FLAG M2 affinity beads (Sigma). The beads collected by centrifugation were washed three times with 1 ml PBS containing protease inhibitor, suspended in 20 μl of sample buffer (0.2 M Tris, 10% sucrose, 10% SDS, and 5 mM EDTA), and incubated at 98°C for 5 min. After centrifugation, the supernatants were electrophoresed through 5–16%

polyacrylamide gradient gels. The gels were subjected to immunoblotting using anti-FLAG polyclonal rabbit antibody (Sigma) or anti-GFP polyclonal rabbit antibody (Sigma) and anti-rabbit or anti-mouse IgG horseradish peroxdase-linked antibody (Amersham Biosciences). The immunoblots were visualized by electrochemiluminescence (Amersham Biosciences).

To determine whether the two GIPRs insert into the ER membrane, the ER-enriched fraction of COS-7 cells cotransfected with the two plasmids (1 μg each) were incubated in PBS containing 0.2 M sucrose in the absence or presence of 0.1 M Na_2CO_3 (pH 10.5) for 1 h on ice. After centrifugation at 100,000 *g* for 30 min, Western blot was performed with the supernatant and pellet using an antibody against FLAG or GFP.

Measurement of insulin secretion and intracellular cAMP production in isolated islets. Islets were isolated from mice and handpicked under a microscope. For insulin secretion studies, groups of 10 islets were preincubated at 37°C for 30 min in KRBB containing 2.8 mM glucose and 0.2% BSA and gassed with 95% O_2 and 5% CO_2. The islets were incubated at 37°C for 30 min in 0.5 ml of KRBB containing 2.8 mM or 11.1 mM glucose and 0.2% BSA in the absence or presence of high potassium (30 mM KCl). The islets were also incubated at 37°C for 30 min in 0.5 ml of KRBB containing 11.1 mM glucose and 0.2% BSA with or without mouse GIP (10^{-9} or 10^{-7} M) or 5 μM forskolin. Aliquots of the sample buffer were subjected to RIA assay for insulin. To determine insulin content, the islets were homogenized in 0.4 ml acid-ethanol and extracted at 4°C overnight. The acidic extracts were dried and subjected to insulin measurement.

For cAMP production studies, 20 preincubated islets were incubated at 37°C for 30 min in 0.3 ml of KRBB containing 11.1 mM glucose, 0.2% BSA, 1 mM IBMX, and 10 mM HEPES (pH 7.4) with or without 10^{-9} M GIP, 10^{-7} M GIP, or 5 μM forskolin. The incubation was stopped by the addition of 60 μl of 2 M $HClO_4$. The samples were immediately mixed and sonicated in ice-cold water for 4 min. The samples were centrifuged for 4 min at 3,000 *g*, and aliquots (240 μl) were neutralized by 60 μl of 1 M Na_2CO_3 and diluted with 60 μl of 2 M HEPES (pH 7.4). cAMP levels were measured by EIA assay.

Statistical analysis. Values are expressed as means ± SE. Statistical analyses were performed using ANOVA and unpaired student's *t*-test. *P* values <0.05 were considered significant.

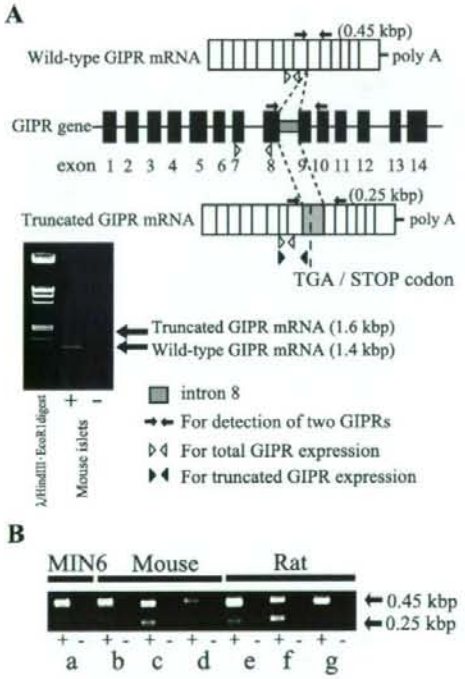

Fig. 1. Structure and expression of the splice variant gastric inhibitory polypeptide (GIP) receptor (GIPR). *A*: the structure of 2 splice variant GIPRs. PCR amplification of mouse (C57BL/6) islet cDNA was performed using COOH-terminal and NH_2-terminal primers of GIPR. The upper band (1.6 kbp) encodes a truncated GIPR isoform that retained the sequence of intron 8 (0.2 kbp) during RNA processing. The lower band (1.4 kbp) encodes wild-type GIPR isoform (full-length GIPR). A minus lane is negative control of mouse islet. The specific primer pair was designed to clearly detect 2 bands of GIPR by RT-PCR (arrows). The primer pair for quantitative RT-PCR to analyze total GIPR expression and truncated GIPR expression is indicated as open arrowhead and filled arrowhead, respectively. Intron 8 is indicated as gray box. *B*: tissue distribution of truncated GIPR in mice, rats, and MIN6 cells. The 0.25-kbp band shows the amplified DNA fragment of wild-type GIPR; the 0.45-kbp band shows that of truncated GIPR. cDNA was prepared from mouse (*a–d*) and rat (*e–f*) tissues, and RT-PCR was performed (*a*, MIN6 cells; *b* and *e*, adipose tissue; *c* and *f*, islets; *d* and *g*, proximal jejunum). A minus lane is negative control of each tissue.

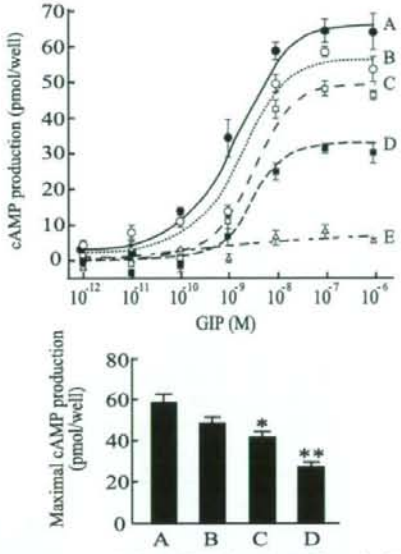

Fig. 2. Dose response analysis of GIP-induced cAMP production in GIPR-expressing COS-7 cells. *Top*: the ratios of the 2 GIPRs were as follows: wild-type GIPR expression plasmid DNA (μg) to truncated GIPR expression plasmid DNA (μg) = 1:0 (●; *A*), 1:0.5 (○; *B*), 1:1 (■; *C*), 1:2 (□; *D*), and 0:1 (△; E). The total amount of plasmid DNA used for each transfection was adjusted to 5 μg by adding pCMV-6c vector. Values are means ± SE. *Bottom*: cAMP induced by 10^{-6} M GIP is shown (n = 3–4). All ED_{50} values of GIP response curves were ~3.0 nM. Values are means ± SE. $^*P < 0.05$; $^{**}P < 0.01$ vs. cAMP induction of wild-type GIPR expression.

RESULTS

Identification of truncated GIPR. PCR amplification and sequencing of full-length GIPR from mouse islet cDNA revealed expression of two isoforms (Fig. 1*A*). The upper band (1.6 kbp) is characterized by unsplicing of intron 8 (0.2 kbp). As a result of the addition, the predicted amino acid reading frame is shifted within the region encoding transmembrane domain 4 and an in-frame stop codon is produced, generating a COOH-terminal truncated form of 263 amino acids desig-

nated as truncated GIPR. The lower band (1.4 kbp) corresponds to full-length GIPR of 460 amino acids designated as wild-type GIPR. To estimate truncated GIPR expression in different tissues, RT-PCR was performed using a different detection primer pair (Fig. 1*B*). Truncated GIPR was expressed not only in mouse islets but also in mouse proximal jejunum and adipose tissue. Truncated GIPR was also expressed in a mouse pancreatic β-cell line (MIN6), rat islets, proximal jejunum, and adipose tissue.

Function of truncated GIPR. To determine the functional properties of truncated GIPR, COS-7 cells were transfected with wild-type and truncated GIPR expression plasmid separately and stimulated with GIP (Fig. 2). In wild-type GIPR-expressing cells, GIP increased cAMP levels in a concentration-dependent manner. In contrast, GIP failed to stimulate cAMP induction in truncated GIPR-expressing cells. COS-7 cells were then cotransfected with wild-type and truncated GIPR expression plasmids. As the amount of truncated GIPR expression plasmid was increased from 0.5 to 2 μg in the presence of 1 μg of wild-type GIPR expression plasmid, maximal cAMP production induced by GIP was reduced, indicating that truncated GIPR had a dominant negative effect against wild-type GIPR. We examined whether truncated GIPR influenced glucagon-like peptide-1 (GLP-1)-induced cAMP production using GLP-1 receptor-expressing COS-7 cells. GLP-1-induced cAMP production was not decreased in the presence of truncated GIPR (data not shown), indicating that the dominant negative effect of truncated GIPR is specific to GIPR.

To determine how truncated GIPR affects wild-type GIPR in COS-7 cells, we constructed a COOH-terminal FLAG-tagged wild-type GIPR expression plasmid (wild-type GIPR-FLAG) and a COOH-terminal GFP-tagged truncated GIPR expression plasmid (truncated GIPR-GFP). When each of these expression plasmids was transfected into COS-7 cells (Fig. 3*A*, *a* and *b*), wild-type GIPR-FLAG was expressed on the cell surface

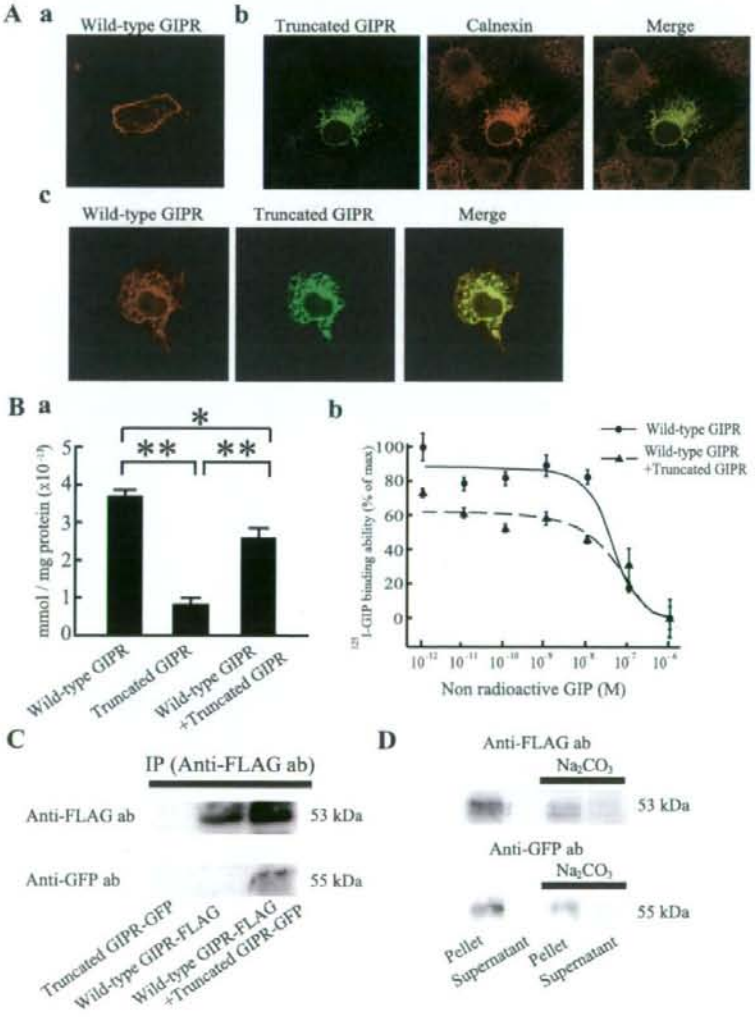

Fig. 3. Cellular localization and interaction of wild-type GIPR and truncated GIPR in GIPR-expressing COS-7 cells. *A*: immunofluorescence staining of the GIPR-expressing COS-7 cells. COS-7 cells were transfected with wild-type GIPR-FLAG (*a*) or truncated GIPR-green fluorescent protein (GFP) (*b*). To estimate localization of truncated GIPR-GFP, anti-calnexin antibody was used as endoplasmic reticulum (ER) maker (green, truncated GIPR-GFP; red, calnexin; yellow, merge). Cotransfection of the 2 GIPRs (*c*) was performed (red, wild-type GIPR-FLAG; green, truncated GIPR-GFP; yellow, merge). Localization of the GIPRs was analyzed by dual wavelength confocal microscopy. We repeated these experiments using 1×10^5 cells 3 times. *B*: binding assay analysis using GIPR-expressing COS-7 cells ($n = 4$; *a*). Competitive GIP binding curves using COS-7 cells transfected with wild-type GIPR (●) or cotransfected with two GIPRs (▲) (wild-type GIPR to truncated GIPR = 1:1 μg, $n = 5$; *b*). The IC_{50} values of binding curves were 5.6×10^{-8} and 7.2×10^{-8} M, respectively. Data are expressed as specific binding to each of the GIPR-expressing cells after subtraction of the specific binding to cells transfected with pCMV-6c vector. Values are means ± SE. $^*P < 0.05$; $^{**}P < 0.01$. *C*: immunoprecipitation and Western blot analysis of ER-enriched fractions of GIPR-expressing COS-7 cells. Immunoprecipitation was performed using anti-FLAG M2 affinity beads. Wild-type GIPR was detected in COS-7 cells transfected with wild-type GIPR alone and cotransfected with the 2 GIPRs using anti-FLAG polyclonal antibody. Truncated GIPR was detected only in COS-7 cells cotransfected with the 2 GIPRs using anti-GFP polyclonal antibody. *D*: Western blot analysis of ER-enriched fractions of the 2 GIPRs-expressing COS-7 cells with or without Na_2CO_3 treatment.

whereas truncated GIPR-GFP expression was limited to the ER, as resolved by anti-calnexin antibody. When both wild-type GIPR-FLAG and truncated GIPR-GFP were coexpressed in COS-7 cells (Fig. 3*A*, *c*), the expression of wild-type GIPR-FLAG on the cell surface decreased and remained highly within the ER. To determine whether the tags of the receptor influenced receptor trafficking, we constructed tag-changed plasmids [a COOH-terminal GFP-tagged wild-type GIPR expression plasmid (wild-type GIPR-GFP) and a COOH-terminal FLAG-tagged truncated GIPR expression plasmid (truncated GIPR-FLAG)] and transfected them into COS-7 cells. Truncated GIPR-FLAG also was located in the ER and decreased wild-type GIPR-GFP trafficking from the ER to the cell membrane (data not shown). We performed a GIP binding assay using COS-7 cells transfected with nontagged wild-type and truncated GIPR. The GIP binding ability of wild-type GIPR was significantly decreased in the presence of truncated GIPR (Fig. 3*B*, *a*). Analysis of GIP binding curves by performing a competitive binding assay showed similar IC_{50} values of both curves (Fig. 3*B*, *b*).

Immunoprecipitation was performed on the prepared ER-enriched fractions of COS-7 cells transfected with the two GIPRs to determine whether truncated GIPR interacts with wild-type GIPR (Fig. 3*C*). In the ER-enriched fraction of cotransfected cells, immunoreactive truncated GIPR-GFP could be detected after immunoprecipitation with the FLAG-tagged wild-type GIPR, indicating that truncated GIPR interacts with wild-type GIPR on the ER membrane. Western blot analysis was performed using the ER-enriched fraction treated by Na_2CO_3 to determine whether the two GIPRs are inserted into the ER membrane (Fig. 3*D*). With Na_2CO_3 treatment peripheral membrane proteins are solubilized into the buffer, whereas integral membrane proteins are insoluble. Two GIPRs were detected in the pellet of the ER-enriched fraction untreated by Na_2CO_3. The two GIPRs were also detected in the pellet of the ER-enriched fraction treated by Na_2CO_3, indicating that the two GIPRs are stably inserted into the ER membrane. Thus, truncated GIPR influenced trafficking of wild-type GIPR from the ER to the cell surface by interacting with wild-type GIPR in the ER.

GIPR sensitivity in islets of HFD mice. To analyze the functional significance of truncated GIPR in vivo, we investigated GIPR sensitivity of β-cells in obese mice induced by high-fat diet. Mice were fed high-fat chow or control fat chow for 10 wk. Body weight was significantly higher in HFD mice compared with CFD mice (37.9 ± 1.8 and 32.3 ± 0.83 g, respectively, $P < 0.05$). To determine the effect of high-fat diet on glucose homeostasis, we carried out OGTTs. Blood glucose levels were similar in HFD and CFD mice (Fig. 4*A*). We then measured plasma insulin levels at the indicated times during OGTTs. Plasma insulin levels were twofold higher in HFD mice at 15 min (1.4 ± 0.2 and 2.7 ± 0.3 ng/ml, respectively, $P < 0.05$), and the area under the curve of insulin secretion during OGTT was significantly increased in HFD mice compared with CHD mice (191.6 ± 21.2 and 130.8 ± 15.8 $ng \cdot ml^{-1} \cdot min^{-1}$, respectively, $P < 0.05$) (Fig. 4*B*). These results suggest compensatory hyperinsulinemia in an attempt to maintain blood glucose levels in high-fat diet-induced obese mice.

To determine sensitivity to GIP in the islets of HFD mice, GIP-induced insulin secretion from isolated islets of these mice

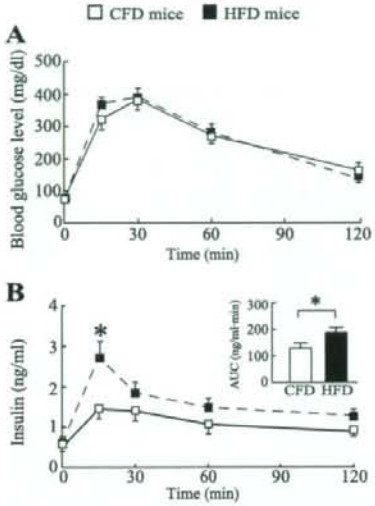

Fig. 4. Oral glucose tolerance tests (OGTTs) in control fat chow (CFD) and high-fat chow (HFD) mice. *A*: blood glucose levels during OGTTs in CFD (□) and HFD (■) mice ($n = 8$). *B*: plasma insulin levels during OGTTs in CFD (□) and HFD (■) mice ($n = 8$). Area under the curves of the insulin secretion during OGTTs in CFD mice (open bar) and HFD mice (filled bar) were also represented. Values are means ± SE. *$P < 0.05$ vs. CFD mice.

was examined in the presence of 11.1 mM glucose, in which incretin can potentiate insulin secretion. Insulin secretion stimulated by 11.1 mM glucose was similar in the islets of CHD and HFD mice (Fig. 5*A*). The islets of HFD mice showed significantly increased insulin secretion in response to 10^{-9} or 10^{-7} M GIP compared with those of CFD mice. On the other hand, forskolin, an adenylate-cyclase activator, increased insulin secretion in islets of CFD and HFD mice to a similar extent. In the presence of 2.8 and 11.1 mM glucose, insulin secretion stimulated by high potassium (30 mM) was also similar in the islets of CFD and HFD mice, respectively (Table. 1). The insulinotropic effect of GIP requires an increase in the level of intracellular cAMP in the β-cells, and cAMP production in the islets of HFD mice was significantly higher than that in CFD mice in the presence of GIP (Fig. 5*B*). However, forskolin increased intracellular cAMP production in the islets of CFD and HFD mice to a similar extent. Thus, GIPR sensitivity to GIP was increased specifically in the islets of HFD mice.

Expression of total and truncated GIPR in islets of HFD mice. To confirm differences in GIPR expression in islets between HFD and CFD mice, quantitative RT-PCR was performed. Total GIPR expression in the islets of HFD mice was similar to that of CFD mice (Fig. 6*A*). The relative expression level of truncated GIPR was then compared in the islets of HFD and CFD mice. The ratio of truncated GIPR to total GIPR expression in the islets of HFD mice was decreased by 32% compared with that in CFD mice (Fig. 6*B*).

DISCUSSION

In the present study, we have identified a novel splice variant GIPR expressed in mouse pancreatic β-cells and characterized its effect on GIPR sensitivity in high-fat diet-induced obese mice.